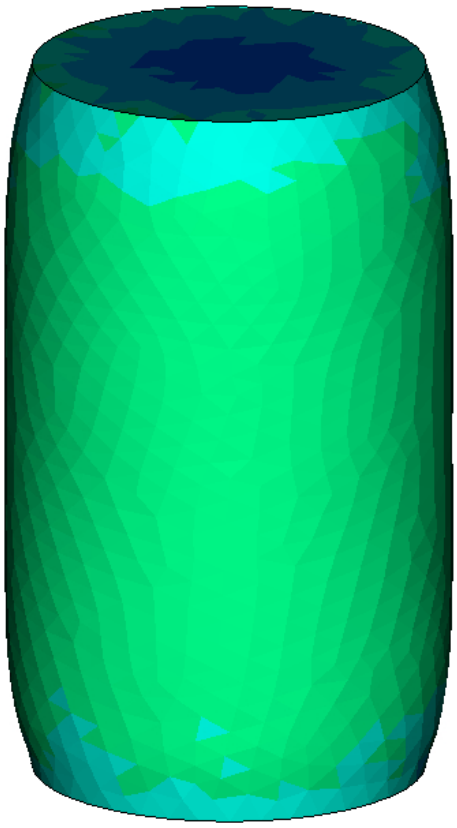

Human centric virtual driven product development

Using FE simulation to compare passive versus active muscle activity for human body model development

Master's thesis in Biomedical Engineering

SIGRID TJERNBERG

DEPARTMENT ELECTRICAL ENGINEERING

CHALMERS UNIVERSITY OF TECHNOLOGY

Gothenburg, Sweden 2024

www.chalmers.se

Master's thesis 2024

Human centric virtual driven product development

Using FE simulation to compare passive versus active muscle activity for human body model development

SIGRID TJERNBERG

Department Electrical Engineering
Signal Processing and Biomedical Engineering
Chalmers University of Technology
Gothenburg, Sweden 2024

Human centric virtual driven product development
Using FE simulation to compare passive versus active muscle activity for human body model development
SIGRID TJERNBERG

Supervisor: Manuel Mendoza Vazquez, Alten Sweden
Examiner: Andreas Fhager, Signal Processing and Biomedical Engineering

Master's Thesis 2024
Department of Electrical Engineering
Signal Processing and Biomedical Engineering
Chalmers University of Technology
SE-412 96 Gothenburg
Telephone +46 31 772 1000

Cover: Pressure map for meshed cylinder entirely made up of muscle tissue being compressed done in BETA CAE systems META.

Typeset in LaTeX
Printed by Chalmers Reproservice
Gothenburg, Sweden 2024

Human centric virtual driven product development
Using FE simulation to compare passive versus active muscle activity for human body model development
SIGRID TJERNBERG
Department of Electrical Engineering
Chalmers University of Technology

Abstract

The aim of this thesis was to gather information about active and passive muscle tissue around the pelvis and use it to simulate the effect on a human body model (HBM). A literature review was conducted in order to find muscle tissue parameters that could be used in the simulation of muscles around the pelvis. Three studies were chosen to compare muscle tissue parameters, the last of which included muscle tissue parameters for both passive and active muscle tissue. The literature review was also conducted to investigate the effects of body mass index (BMI) on the muscle tissue properties. Then two models were designed in order to simulate in vivo and in vitro muscle tissue tests which were used for the first sets of simulations. The first simulations were designed to be done quickly so that several different muscle tissue parameters could be tested effectively and compared. Part of this comparison was to check the material model stability in the range of relevant strains. The last step was to implement the muscle tissue parameters in a HBM and see how it affected the model. The results showed that there is a lack of information within the field and a lot of misinformation where bad values were being used, however a few studies which were deemed as good which had parameters which could be used in ABAQUS FEA were summarized in this thesis. All these muscle tissue parameters were tested on the cylinder designs which resulted in force-displacement plots which could be compared to each other. Active and passive muscle material parameters were then applied to a HBM which resulted in two different models which were compared. The conclusion of the thesis showed that active versus passive tissue does affect the HBM.

Keywords: FE, HBM, muscle tissue, active muscles, passive muscles, ABAQUS

Acknowledgements

I would especially like to thank my supervisor Manuel Mendoza-Vazquez for the patience, support and guidance throughout the entire course of the project. A big thanks to the team there as well for giving me the chance and opportunity to pursue this project and for all the help and rewarding discussions along the way.

I would also like to thank my examiner Andreas Fhager for taking on this project and for the help during this period.

Finally, I would like to thank my family and friends for their support throughout the project.

Sigrid Tjernberg, Gothenburg, June 15, 2024

List of Acronyms

Below is the list of acronyms that have been used throughout this thesis listed in alphabetical order:

3D	Three dimensional
AWT	Abdominal wall tension
BMI	Body mass index
CC	Contractile component
EAO	External abdominal oblique
FE	Finite Element
HBM	Human-Body Model
IAO	Internal abdominal obliques
IAP	Intra-abdominal pressure
MR	Magnetic resonance imaging
MTP	Muscle tissue parameters
PEC	Parallell elastic component
RA	Rectus abdominus
SEC	Series elastic component
TA	Transversus abdominis

Nomenclature

Below is the nomenclature of parameters that have been used throughout this thesis.

Parameters

F_{CC}	Force generated by contractile component
F_{PEC}	Force generated by parallel elastic component
F_{SEC}	Force generated by series elastic component
F	Deformation gradient
x	Current position
X	Reference position
J	Total volumetric change
$\bar{F}^{def}$	Deformation gradient without volumetric change
$\bar{B}$	Deviatoric stretch tensor
$\bar{I}_i$	Strain invariants
δL	Displacement gradient
u	Displacements
δD	Virtual rate of deformation
$\delta \epsilon^{vol}$	Virtual volumetric strain rate
δe	Virtual deviator strain rate
U	strain energy potential
C_{ij}	Temperature dependent material parameter
D_i	Temperature dependent material parameter
J_{el}	Elastic volume strain
J_{th}	Thermal volume strain
μ_i	Material parameter used in ogden model
α_i	Material parameter used in ogden model
λ	principal stretches of deformation tensor

ν	Poisson´s ratio
k_i	Material parameters

Contents

List of Acronyms **ix**

Nomenclature **xi**

List of Figures **xv**

List of Tables **xix**

1 Introduction **1**
1.1 Background 1
1.2 Objectives 2
1.3 Limitations 2

2 Theory **3**
2.1 Muscle structure 3
2.1.1 Anatomy 4
2.2 Models 8
2.2.1 Hills muscle model 8
2.2.2 Material models 10
2.2.3 FE HBM 12

3 Literature review **15**
3.1 Data gathering 15
3.2 Results 16
3.2.1 Body type 16
3.2.2 Material property values 17

4 Methods **21**
4.1 Cylinder design 21
4.2 HBM 23

5 Simulation **25**
5.1 Cylinder tests 25
5.1.1 Model verification 25
5.1.2 Phase 1 25
5.1.3 Phase 2 26
5.2 Human body model test 26

6 Results **27**
6.1 Literature review . . . 27
6.2 Simulation . . . 28
6.2.1 Cylinder . . . 28
6.2.2 Human body model . . . 37

7 Discussion **39**
7.1 Method . . . 39
7.2 Literature review . . . 39
7.3 Simulation results . . . 40
7.3.1 Cylinder . . . 40
7.3.2 HBM . . . 41

8 Conclusion **43**

A Appendix A **I**
A.1 Stiffness values . . . I

B Appendix B **III**
B.1 Force-displacement curves in vitro values . . . III
B.2 Force-displacement curves Active versus passive muscle tissue values . IV

List of Figures

2.1 "File:1007 Muscle Fibes (large).jpg" from Wikimedia Commons by OpenStax, license: Creative Commons Attribution 4.0 International. An illustration showing the structure of muscles. 4

2.2 "File:1112 Muscles of the Abdomen.jpg" from Wikimedia Commons by OpenStax, license: Creative Commons Attribution 4.0 Internationa. Illustration of abdominal muscles. 5

2.3 Hill muscle model where SEC is the first elastic component, PEC is the second elastic component which is in parallel with CC which is the contractile component. 9

2.4 Simpler version of the Hill muscle model where SEC and PEC are the elastic component and CC is the contractile component. 9

3.1 Infographic of how data gathering and selection was done. At the start when only using key search words there were 1228 sources available and at the end only 5 sources were actually usable. 15

4.1 Cylinder designed and meshed with Then C. et al. study *A method for a mechanical characterisation of human gluteal tissue*, muscle size as inspiration. In the upper right corner a small working plane can be seen, green points towards y-direction, blue towards z-direction and red towards x-direction. 22

4.2 Cylinder designed and meshed to imitate in vitro studies with design inspiration from Then C. et al. study *A method for a mechanical characterisation of human gluteal tissue* and Hernández B. et al. study *Mechanical and histological characterization of the abdominal muscle. A previous step to modelling hernia surgery.* In the upper right corner a small working plane can be seen, green points towards y-direction, blue towards z-direction and red towards x-direction. 23

6.1 The resulting force-displacement curves from 30mm indentation testing on solid muscle where the blue graph is with muscle tissue properties taken from Table 6.1 MTP 1 and the orange graph is with muscle tissue properties from Table 6.1 MTP 2. The dashed line is approximated from *A method for a mechanical characterisation of human gluteal tissue* which is where MTP 1 came from. 29

6.2 The Cylinder to the left is equiped with the muscle tissue parameters found in Table 6.1 MTP 1 and the cylinder to the right is equipped with the muscle tissue parameters found in Table 6.1 MTP 2. 30

6.3 The resulting internal energy curves from 30mm indentation testing on solid muscle where the blue graph is with muscle tissue properties taken from Table 6.1 MTP 1 and the orange graph is with muscle tissue properties from Table 6.1 MTP 2. 31

6.4 The upper two dashed lines is the in vitro design of the cylinder being indented and the bottom two graphs shows the in vivo cylinder being indented. The blue graphs are from muscle tissue parameters found in Table 6.1 MTP 1 and the orange graphs is with the muscle tissue parameters found in Table 6.1 MTP 2. 32

6.5 The Cylinder to the left is the in vivo cylinder and the cylinder to the right and below is the in vitro cylinder both with muscle tissue parameters found in Table 6.1 MTP 1. 33

6.6 Force-displacement plots for all seven subjects with both relaxed (R) and tense (T) muscles. The muscle parameter values are taken from Table 6.1 MTP 3 and the cylinder design inspired from *A method for a mechanical characterisation of human gluteal tissue*. The graphs with tense muscle tissue is illustrated with dashed lines whilst the relaxed tissue is illustrated with solid lines. 34

6.7 Zoomed in force-displacement plots for subject one with both relaxed (R) and tense (T) muscles. The muscle parameter values are taken from Table 6.1 MTP 3 and the cylinder design inspired from *A method for a mechanical characterisation of human gluteal tissue*. 35

6.8 The Cylinder to the left is the simulated relaxed muscle tissue of subject one and the cylinder to the right is the simulated tense muscle tissue of subject one both under the maximum amount of indentation. Muscle tissue parameter values are taken from Table 6.1 MTP 3. . . . 35

6.9 Zoomed in force-displacement plots for subject two with both relaxed (R) and tense (T) muscles. The muscle parameter values are taken from Table 6.1 MTP 3 and the cylinder design inspired from *A method for a mechanical characterisation of human gluteal tissue*. 36

6.10 The Cylinder to the left is the simulated relaxed muscle tissue of subject two and the cylinder to the right is the simulated tense muscle tissue of subject two both under the maximum amount of indentation. Muscle tissue parameter values are taken from Table 6.1 MTP 3. . . . 36

B.1 Force-displacement plots of both in vivo and in vitro cylinder designs with muscle tissue material values taken from Tomaszewska A. et al. study. III

B.2 Force-displacement plots of subject one with both relaxed (R), in blue, and tense (T), in orange, muscles. The muscle parameter values are taken from Table 6.1 MTP 3 and the cylinder design inspired from Then C. et al. study *A method for a mechanical characterisation of human gluteal tissue.* The first image is to scale with all others and the second is zoomed in. IV
B.3 Force-displacement plots of subject two with both relaxed (R), in blue, and tense (T), in orange, muscles. The muscle parameter values are taken from Table 6.1 MTP 3 and the cylinder design inspired from Then C. et al. study *A method for a mechanical characterisation of human gluteal tissue.* The first image is to scale with all others and the second is zoomed in. V
B.4 Force-displacement plots of subject three with both relaxed (R), in blue, and tense (T), in orange, muscles. The muscle parameter values are taken from Table 6.1 MTP 3 and the cylinder design inspired from Then C. et al. study *A method for a mechanical characterisation of human gluteal tissue.* The first image is to scale with all others and the second is zoomed in. VI
B.5 Force-displacement plots of subject four with both relaxed (R), in blue, and tense (T), in orange, muscles. The muscle parameter values are taken from Table 6.1 MTP 3 and the cylinder design inspired from Then C. et al. study *A method for a mechanical characterisation of human gluteal tissue.* The first image is to scale with all others and the second is zoomed in. VII
B.6 Force-displacement plots of subject five with both relaxed (R), in blue, and tense (T), in orange, muscles. The muscle parameter values are taken from Table 6.1 MTP 3 and the cylinder design inspired from Then C. et al. study *A method for a mechanical characterisation of human gluteal tissue.* The first image is to scale with all others and the second is zoomed in. VIII
B.7 Force-displacement plots of subject six with both relaxed (R), in blue, and tense (T), in orange, muscles. The muscle parameter values are taken from Table 6.1 MTP 3 and the cylinder design inspired from Then C. et al. study *A method for a mechanical characterisation of human gluteal tissue.* IX
B.8 Force-displacement plots of subject seven with both relaxed (R), in blue, and tense (T), in orange, muscles. The muscle parameter values are taken from Table 6.1 MTP 3 and the cylinder design inspired from Then C. et al. study *A method for a mechanical characterisation of human gluteal tissue.* IX

List of Tables

2.1 Muscle groups looked at around the abdomen with names, placements and roles. The Pyramidalis is included in this table but not large enough to be relevant for our subject. 6
2.2 Overview of muscle groups around the hip, pelvis, and buttocks, including names, placements and roles. 7
2.3 Muscle groups examined around the thigh, with names, placements and roles. 8

6.1 Summarized values of MTPs from three different sources. The first one being an Ogden material model from *A method for a mechanical characterisation of human gluteal tissue* by Then C. et al.. The second one being an Holzapfel-Gasser-Ogden material model by Then C. et al. called *Method for characterizing viscoelasticity of human gluteal tissue*. The third, which also used a Ogden model, called *Combining Freehand Ultrasound-Based Indentation and Inverse Finite Element Modeling for the Identification of Hyperelastic Material Properties of Thigh Soft Tissues* done by Fougeron N. et al.. 27

A.1 Different levels of activity in abdominal muscles and the Holzapfel-Gasser-Ogden material parameters I
A.2 Summary of Mechanical Properties of Abdominal Tissues I
A.3 Mechanical Properties of Various Tissues II
A.4 Muscle tissue values of the abdomen II

1
Introduction

Incontinense affects around 300 million people worldwide which is around 5% of the population [1]. However in this 70 billion dollar industry, almost none of the tests of diapers mention comfort as a criteria. 300 million people use diapers and to explore a more efficient way to improve product-user interaction which excludes early on human testing could make a huge difference to the industry.

A leading personal hygiene company has started to develop human body models to improve product user interactions which are called avatars. Extensive research has been done to create a model which imitates the human body. However, the soft tissue of a human body is very complex especially when looking at skeletal muscle and tendons which differ in size and stiffness based on level of activity, positioning of the body and over all between different individuals. In the current avatars muscles are modeled as passive but the objective of this thesis was to figure out the difference in product to user interaction when replacing the current muscle tissue with active muscle tissue.

When looking into different muscles and their parameters the pelvic area was divided into four different categorizes, abdominal , pelvis, hip and thigh muscles. This division was done due to many anatomical studies and models which has been done on only one area. These various studies and models have been summarized and applied to a model.

1.1 Background

When testing absorbing hygiene products today, companies often choose to do laboratory testing and testing on mannequins [2] [3]. To create a human body model (HBM) where product-user interaction is tested could potentially ease the stress of the laboratory work and improve hygiene product to be more comfortable for users whilst also improving the functionality of the product. This also allows for testing of design concepts early in the design cycle, when no products are available.

When looking into different HBM´s, using Hill´s muscle model is the most common way to model muscles [4]. This model considers the contractile and the elastic elements of muscles. To improve a detailed virtual HBM utilizing the finite element (FE) approach was the main focus in this study. Research in human anatomy and real life muscle functions was conducted in order to improve the current FE HBM.

Many models today are very focused on specific areas many times to predict injuries in accidents or crashes where the model parameters are very extreme whereas this study focused on the daily muscle parameters.

One of the latest FE models done for the abdominal muscles was conducted by Jourdan A. et al [5] and will be looked at during this project. The aim of this study was to create a FE generated pelvic area with muscle activation in order to test product-user interactions. This will be done by focusing on the effects of muscle stiffness when a displacement of muscular tissue is created with an external pressure source.

1.2 Objectives

The aim of this thesis was to evaluate the difference in product to user interaction when considering muscle tissue as active. This involves:

1. Literature review on how stiffness in muscles changes with level of activity. This includes looking into articles that have studied and modelled active muscles in FE.
2. Literature review on how level activity in muscles changes depending on body position and body type.
3. Simulate a product user interaction case with passive and active muscles and study the differences in a HBM.

These objectives were created to test how the stiffness and activity of muscles, discovered during the literature review, would affect a HBM once an external pressure was applied. This would in turn help with understanding the product-user interaction in the pelvic area during different activities in day to day life.

1.3 Limitations

The limitations of this project include only looking at muscle tissue and no other tissue parameters in the body. I did not look into other parts of the human body that changes during activity or positioning. Another limitation was that I only worked with one adult model, the effect of muscle activity could be different between adults due to different muscle properties such as muscle size or amount of fat tissue.

2

Theory

This project looked at a new but current area where biology and programming/simulation meet. This project therefore requires a good understanding of both fields to understand the studies and the models. In vitro and in vivo experiments were studied and also current FE HBM models to try and combine into new models which imitate the human body. In this theory both human biology and current models will be discussed to give thorough knowledge of the field.

2.1 Muscle structure

The review article "Morphological and Functional Aspects of Human Skeletal Muscle" by Trovato F. et al [6] provides a comprehensive overview of skeletal muscle and its development, structure, function, and its overall role in the body. Skeletal muscle constitutes around 40% of the body weight and contains 50-75% of the body's proteins and is crucial for movement and posture. Healthy skeletal muscle is crucial for preventing diseases and maintaining well-being [6].

A representation of skeletal muscle and its different parts can be seen in Figure 2.1. Skeletal muscle is composed of muscle cells, myoblasts, which are grouped into muscle fibers which in turn are grouped into muscle fascicles. The muscle fascicles are then also grouped to form the skeletal muscle [6]. Surrounding the entire skeletal muscle, muscle fascicles and muscle fibers is the epimysium, perimysium and endomysium respectively. The connective tissue helps innerve and vascularize the tissue which makes the muscles function [6]. When the muscle tenses the muscle fibers contract which leads to a contraction of the entire muscle and when this happens the muscle becomes stiffer.

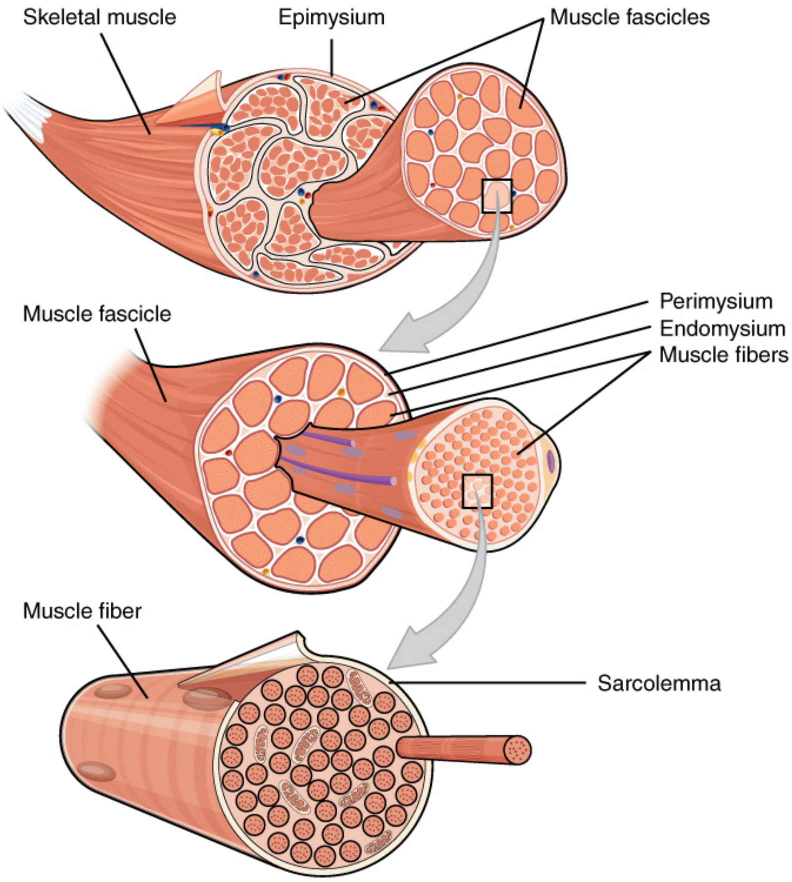

Figure 2.1: "File:1007 Muscle Fibes (large).jpg" from Wikimedia Commons by OpenStax, license: Creative Commons Attribution 4.0 International. An illustration showing the structure of muscles.

2.1.1 Anatomy

The human anatomy of the pelvic area plays a huge role in the muscle modeling since we are trying to mimic the model to be as close to reality as possible but without doing unnecessary details. Looking at Figure 2.2 there are a lot of muscles and ligaments and for our model we will divide these muscles into groups. The three main groups will be the abdomen, hip and thigh areas. Different studies have looked in to different areas and these will be discussed further down under each section below.

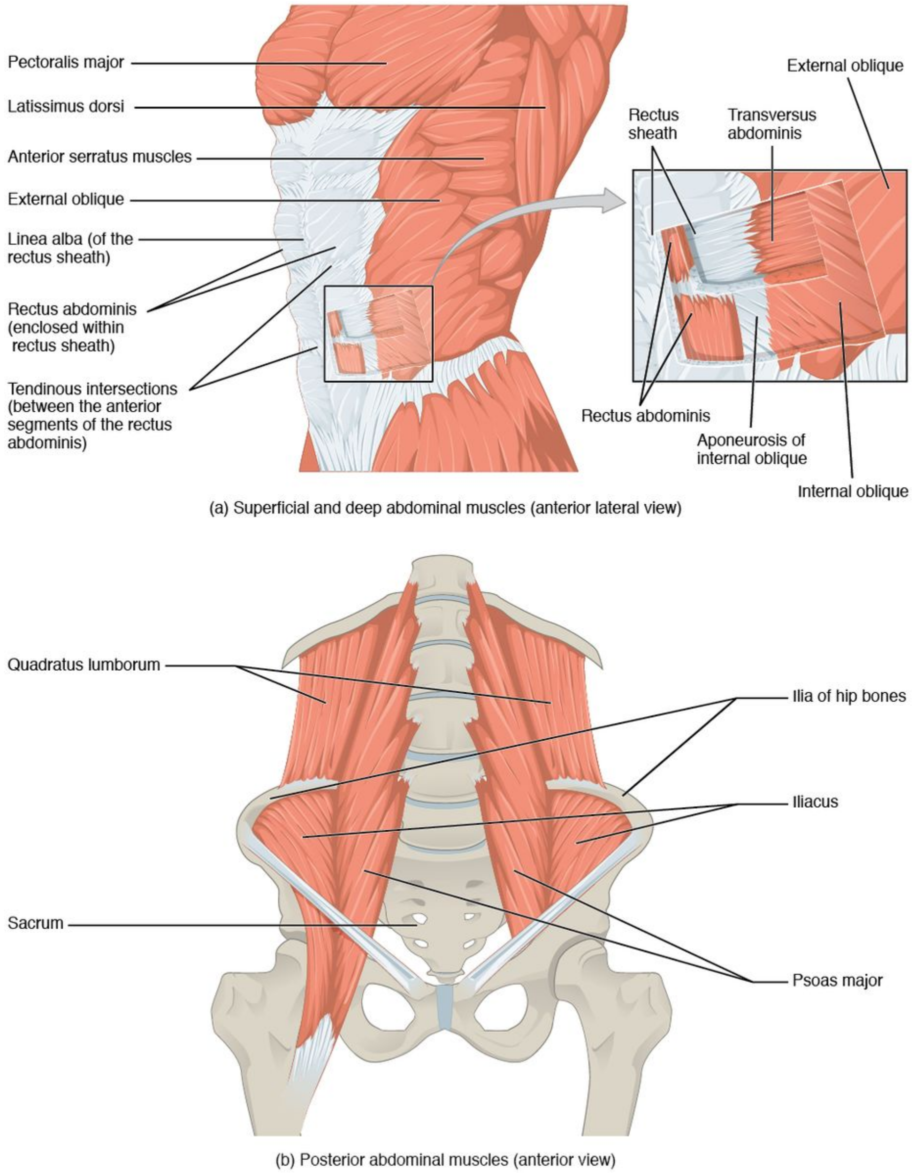

Figure 2.2: "File:1112 Muscles of the Abdomen.jpg" from Wikimedia Commons by OpenStax, license: Creative Commons Attribution 4.0 Internationa. Illustration of abdominal muscles.

Abdomen

There are five main muscle groups around the abdomen. Their names, placement and functions are presented in Table 2.1. Information in the table is gathered from *Anatomy, Abdomen and Pelvis: Abdominal Wall* [7].

Table 2.1: Muscle groups looked at around the abdomen with names, placements and roles. The Pyramidalis is included in this table but not large enough to be relevant for our subject.

No	Name	Insertion	Action
1	Pyramidalis	Attaches between the pubic symphysis and pupic crest and goes to the line alba	Contract with abdominal muscles to increase positive pressure. Connected with posture
2	Rectus abdominus (RA)	Attaches by the pupic crest and goes to the xiphoid and costal cartilage	It is one of the most superficial muscle in the abdomen and the main functions are, flexion of the trunk and core stability
3	External abdominal oblique (EAO)	Attaches by the pubic tubercle and iliac crest and goes to the lower eight ribs on the lateral side of the body	It is one of the most superficial muscles in the abdomen and the main functions are, rotation of the trunk and core stability
4	Internal abdominal obliques (IAO)	Attaches by the pubic crest and goes to the lower four ribs on the lateral side of the body	The main function is the flex the trunk which leads to increased intraabdominal pressure (IAP)
5	Transversus abdominis (TA)	Attaches by the iliac fascia, inguinal ligament, iliac crest, thoracolumbar fascia and the lower seven ribs and goes to the linea alba, IAO, pubic crest and the pectinal line of pubis	The main functions is to keep abdominal tension and increase IAP when doing forceful expirations.

Hip

The muscles of the hip is presented in Table 2.2 and the data is gathered from *Hip and thigh muscles* [8].

Table 2.2: Overview of muscle groups around the hip, pelvis, and buttocks, including names, placements and roles.

No	Name	Insertion	Action
1	Gluteus Maximus	Attaches to the gluteal tuberosity of the femur and iliotibial tract.	Major extensor of the thigh and is important for climbing and running.
2	Gluteus Medius	Attaches to the lateral surface of the greater trochanter of the femur.	Abducts and medially rotates thigh and stabilizes pelvis during walking.
3	Gluteus Minimus	Situated below the gluteus medius and attaches to the anterior of the greater trochanter.	Similar to gluteus medius it helps in abduction and medial rotation of the thigh.
4	Tensor Fasciae Latae	Iliotibial band to the Gerdy's tubercle on the lateral tibia.	Stabilizes the hip and knee and assists in thigh abduction.
5	Obturator Internus	Attaches to the greater trochanter of the femur.	Rotates the thigh and stabilizes the hip joint.
6	Obturator Externus	Attaches to the trochanteric fossa of the femur.	Helps with rotation of the thigh.
7	Gemellus Superior	Next to the obturator internus and attaches to the greater trochanter.	Works with obturator internus with rotatation of the thigh.
8	Gemellus Inferior	BSituated below the gemellus superior and attaches to the greater trochanter.	Helps with rotation of the thigh and stabilizes the hip.
9	Quadratus Femoris	From ischial tuberosity to the trochanteric crest of the femur.	Rotates the thigh and helps with stabilization of the hip joint.
10	Piriformis	Attaches from the anterior part of the sacrum to the greater trochanter of the femur.	Rotates the thigh at the hip joint.
11	Iliopsoas (Iliacus and Psoas Major)	Psoas major attaches from the lesser trochanter of the femur and Iliacus and attaches to the iliac fossa.	The primary flexor of the thigh and is crucial for walking and running.

Thigh

The thigh consists of eight muscles which has been simplified to three muscle groups, Quadriceps Femoris (Anterior), Adductor Magnus (Medial) and Hamstrings (Posterior). Information about these different muscles can be found in Table 2.3 and was gathered from data is gathered from *Physiopedia* [9].

Table 2.3: Muscle groups examined around the thigh, with names, placements and roles.

No	Name	Insertion	Action
1	Quadriceps Femoris (Anterior)	Attaches to the patella via the quadriceps tendon and then to the tibial tuberosity via the patellar ligament.	Primarily responsible for leg extension at the knee and is critical for walking, running, jumping, and squatting.
2	Adductor Magnus (Medial)	Attaches to the femur's linea aspera and the medial epicondyle of the femur.	Adducts and medially rotates the thigh and plays a significant role in stabilizing the pelvis.
3	Hamstrings (Posterior)	Attach from the ischial tuberosity on the pelvis to various locations on the tibia and fibula.	Involved in knee flexion and hip extension and is essential for walking, running, and jumping.

2.2 Models

This section will describe the different models that were looked at during this project. In the first part the Hills muscle model was looked at which is used to describe the mechanical properties of muscle. In the second part different material models was looked at which can describe the characteristics of muscle tissue and specific parameters that are used by different levels of complex models to describe the intricate tissue that is muscles. The third, and last part, looked at FE HBM which can be used to analyse the entirety of the musculoskeletal system and the different software which can be used.

2.2.1 Hills muscle model

Hills muscle model is a model to describe the mechanical properties of muscle and is composed of three parts. Two elastic components, SEC (Series Elastic Component) and PEC (Parallel Elastic Component), and one contractile component (CC). This can be seen in Figure 2.3.

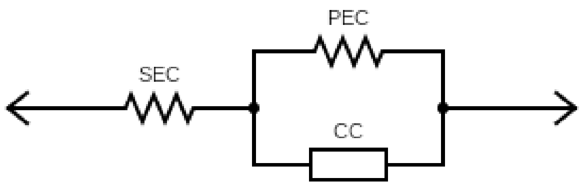

Figure 2.3: Hill muscle model where SEC is the first elastic component, PEC is the second elastic component which is in parallel with CC which is the contractile component.

The CC describes the part of the muscle that actively produces force when activated. The force that CC produces is expressed along the muscle including SEC which is often looked at as the tendon-muscle elasticity [4]. PEC is used to describes the passive force that muscles have during rest due to the material properties of muscle (they are never slack)[4]. The goal of this project in relation to the Hill muscle model is to determine the difference between the CC and the PEC forces and how it correlates to the appearance of the muscles, size and stiffness.

The Hill muscle model can also be modeled as seen in 2.4 where SEC is instead in series with only the CC and not the PEC which is a simpler way of looking at the muscle but not as accurate.

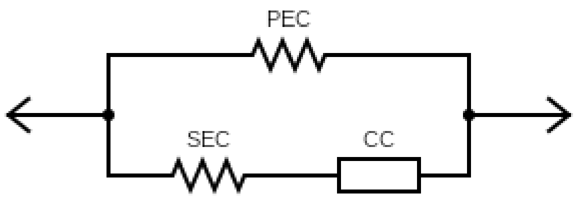

Figure 2.4: Simpler version of the Hill muscle model where SEC and PEC are the elastic component and CC is the contractile component.

However in some instances this model is much easier to work with and generate similar results and can therefor often be used in muscle modeling.

The differences in force equations between the complex and simple Hill muscle modeled can be seen in equation 2.1 and equation 2.2. The first being the complex and the second the simple muscle model.

$$(F_{CC} + F_{PEC})cos\theta = F_{SEC} \tag{2.1}$$

$$F_m = F_{PEC} + F_{SEC} = F_{PEC} + F_{CC}cos\theta \tag{2.2}$$

F_{CC} is the force generated by the CC, F_{PEC} is the force generated by the PEC, θ is the angle between the CC and SEC, F_{SEC} is the force generated by the SEC and

F_m (only for simple model) is the force over the entire muscle. This is the force that goes in line with the muscle and for this project the main focus will be on the transversal muscle force and stiffness however many muscle models that will be looked at are using the basis of Hill muscle modeling.

2.2.2 Material models

There are different types of material models that can be used to model muscles, in this project the focus will be on hyperelastic material models which will be discussed below. The reason for this is due to their complexity and their ability to accurately capture the complex nonlinear behavior of the tissue. Before going in to specific material models and their pros and cons there are some functions which all the models have in common.

For starters the deformation gradient F can be defined as

$$F = \frac{\partial x}{\partial X} \tag{2.3}$$

where x is the current position of the material point and X is the reference position of the same point. From this equation the total volumetric change can be defined as follows [10].

$$J = det(F) \tag{2.4}$$

Then the deformation gradient without volumetric change can be defined as follows.

$$\overline{F}^{def} = J^{-\frac{1}{3}} F \tag{2.5}$$

There are two stretch tensors included in hyperelastic materials, there is the volumetric which can be found in equation 2.4 and the deviatoric. The deviatoric stretch tensor (the left Cauchy-Green strain tensor) which occurs when a material deforms without changing volume and has the following equation [10].

$$\overline{B} = \overline{F} \cdot \overline{F}^T \tag{2.6}$$

From these definitions we can define the first two strain invariants $\overline{I}_1$ and $\overline{I}_2$.

$$\overline{I}_1 = trace\overline{B} = I : B \tag{2.7}$$

$$\overline{I}_2 = \frac{1}{2}\left(\overline{I}_1^2 - trace(\overline{B} \cdot \overline{B})\right) = \frac{1}{2}\left(\overline{I}_1^2 - I : \overline{B} \cdot \overline{B}\right) \tag{2.8}$$

To continue the displacement gradient, δL, which defines how much the displacement of a point changes as it moves around within the material, can be defined as follows [10].

$$\delta L = \frac{\partial \delta u}{\partial x} \tag{2.9}$$

where u are the displacements. To calculate the virtual rate of deformation the following equation can be used where only the symmetric part of the displacement gradient is taken [10].

$$\delta D = sym(\delta L) = \frac{1}{2}(\delta L + \delta L^T) \tag{2.10}$$

From the virtual rate of deformation the virtual volumetric and deviatoric strain rates, $\delta\varepsilon^{vol}$ and δe, can be defined [10].

$$\delta\varepsilon^{vol} = I : \delta D \tag{2.11}$$

$$\delta e = \delta D - \frac{1}{3}\delta\varepsilon^{vol} I \tag{2.12}$$

Given all of these equations definitions the general formulation for strain energy potential, U, can be written as equation 2.13.

$$U = f(\overline{I}_1 - 3, \overline{I}_2 - 3) + g(J_{el} - 1) \tag{2.13}$$

Where the function f can be seen as an expanding Taylor series and g is defined as follows [10].

$$g(J_{el} - 1) = \sum_{i=1}^{N} \frac{1}{D_i}(J_{el} - 1)^{2i} \tag{2.14}$$

This gives us the following equation

$$U = \sum_{i+j=1}^{N} C_{ij}(\overline{I}_1 - 3)^i(\overline{I}_2 - 3)^j + \sum_{i=1}^{N} \frac{1}{D_i}(J_{el} - 1)^{2i} \tag{2.15}$$

In equation 2.15 C_{ij} and D_i are two temperature dependent material parameters. J_{el} is the elastic volume strain and derives from the total volume strain J and the thermal volume volume strain J_{th} with the relation found in equation 2.16

$$J_{el} = \frac{J}{J_{th}} \tag{2.16}$$

where J_{th} can be calculated with the following equation [10].

$$J_{th} = (1 + \varepsilon_{th})^3 \tag{2.17}$$

Neo-Hookean

The Neo-Hookean hyperelastic model is the simplest model that will be looked into in this project and is defined by equation 2.18 [11].

$$U = C_{10}(\overline{I}_1 - 3) + \frac{1}{D_1}\left(J^{el} - 1\right)^2 \tag{2.18}$$

This equation is derived from equation 2.15 where N=1 and the second invariant $\overline{I}_2$, affect on the tissue has been disregarded. In practice this means that the material parameters are the same in all directions which might not be accurate for muscles under larger strain.

Mooney–Rivlin

The Mooney-Rivilin hyperelastic model is derived from equation 2.15 as well but here both invariants of the left Cauchy-Green tensor are acconted for. N=1 in this model as well which gives the following equation [11].

$$U = C_{10}(\bar{I}_1 - 3) + C_{01}(\bar{I}_2 - 3) + \frac{1}{D_1}\left(J^{el} - 1\right)^2 \tag{2.19}$$

This can give a more accurate model than the Neo-Hookean but both of these models will still give similar accuracy since they are of the same order since neither of them can not represent the upturn in the stress-strain curve at higher strain levels.

Yeoh hyperelastic model

To better model the previously mentioned upturn the Yeoh hyperelastic model can be used where the j coefficient is equal to zero and N is equal to three. This gives the following equation [11].

$$U = C_{10}(\bar{I}_1-3)+C_{20}(\bar{I}_1-3)^2+C_{30}(\bar{I}_1-3)^3+\frac{1}{D_1}\left(J^{el}-1\right)^2+\frac{1}{D_2}\left(J^{el}-1\right)^4+\frac{1}{D_3}\left(J^{el}-1\right)^6 \tag{2.20}$$

The second invariant, I_2 is hard to measure and is therefore neglected. It also makes for a relatively accurate and easier to use model.

Ogden hyperelastic model

The Ogden hyperelastic model has the following equation. [11].

$$U = \sum_{i=1}^{N} \frac{2\mu_i}{\alpha_i^2}\left(\lambda_1^{-\alpha_i} + \lambda_2^{-\alpha_i} + \lambda_N^{-\alpha_3} - 3\right) + \sum_{i=1}^{N} \frac{1}{D_i}\left(J^{el} - 1\right)^{2i} \tag{2.21}$$

In this equation μ and α are material parameters and λ is the principal stretches of the deformation tensor. The Ogden model is a very powerful model but can be seen as pretty complex where it can be difficult to chose the material parameters [12]. Ogden is also used for incompressible materials which were a majority of the materials looked at in this study.

2.2.3 FE HBM

This project focused on FE HBM and there were a few alternatives to consider for the goal of this project.

ABAQUS FEA

Positives:

1. Powerful Finite Element Analysis: ABAQUS FEA is a powerful finite element analysis software suite, offering complex and accurate analysis. [13]
2. Accurate Impact Analysis: Provides accurate impact and dynamic analysis which was simulated in this study. [13]

3. Python compatibility: Python codes can be integrated in the analysis making the software easier to navigate and create on script which can be used multiple times. [13]

Negatives:

1. Complex: The software can be hard to understand and takes some time to learn. [13]
2. Expensive: The program is quite expensive. [13]

OpenSim

Positives:

1. User-Friendly Interface: Intuitive interface for creating musculoskeletal models, making it very accessible.
2. Many available models: The users of the software can post models and updates leading to a huge library of models.
3. Dynamic Simulations: OpenSim offers advanced capabilities for dynamic simulations, allowing users to study muscle activations, joint kinematics and dynamic movements.

Negatives:

1. Limited Muscle Volume Representation: Currently the software lacks built-in tools for accurately representing muscle volumes in all parts of the musculoskeletal system.
2. Customization: While OpenSim provides flexibility for customization, the published models are done by the user where it can be hard to track down the references used which makes the results hard to confirm.

CLO

Prositives:

1. User-Friendly: The software is very intuitive and user-friendly with finished models and movement patterns making it very accessible.
2. Customization Options: The software provides customization options for virtual avatars, allowing simulations of different costumed garments and also passive and active muscles.
3. Short Processing Time: Efficient processing is something found with this software, resulting in relatively short simulation times and quick feedback.

Negatives:

1. Data Restrictions: Access to data and material property sources is limited, which makes the results hard to confirm.
2. Limited Accuracy: The results obtained from CLO simulations did not always accurately represent real-world fit, affecting the reliability of the software for research purposes.

After this comparison was done between different softwares ABAQUS FEA was chosen to move forward with in this project. The biggest reason for this was the ability to customize muscle tissue properties and the over all reliability.

3

Literature review

The literature reviews goal was to look into muscle characteristics for different body types and effects on muscle stiffness values during activities. The review was done in different parts, the first part was to look into muscle characteristics for different body types and the second was to find out how different levels of activity affects different muscle groups.

3.1 Data gathering

The data gathering was conducted using a few key search words in order to get as much information as possible within the field to answer the two first objectives which can be found under Section 1.2. All data was gathered from Chalmers Library and an example of how the selecting was done can be seen in the following illustration.

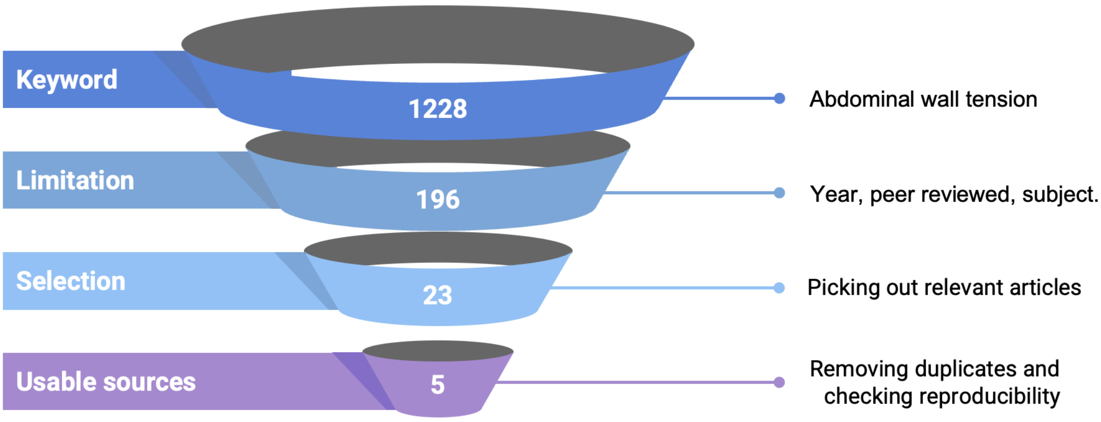

Figure 3.1: Infographic of how data gathering and selection was done. At the start when only using key search words there were 1228 sources available and at the end only 5 sources were actually usable.

When only using the key search word "Abdominal wall tension" the database finds 1228 sources, this was limited to have been published within the last 20 years, be peer reviewed, be within the subject of the abdominal wall, left was 196 articles. These articles were browsed through and 23 of them were deemed relevant. When then reading through these more carefully and looking for reproducibility, duplicates and credibility there were only five articles which were suitable for this project. Similar selections were done for eight different key search words which can be found listed below.

- Abdominal wall tension (AWT)
- Abdominal wall displacement
- Finite element trunk muscles
- Finite element pelvic muscles
- Finite element thigh muscles
- Tissue compliance gluteus
- Gluteus tension displacement

This reviews purpose was only to look for the stiffness of muscle tissue in the transverse plane (outwards direction from the body). Many sources looking at muscle strength, stretch or which tried to simulate muscles in the longitudinal direction was therefore instantly disregarded. The reproducibility criteria in the funnel refers to other HBM or tissue models where the simulations could not be redone due to lack of information. The usable sources was a mix between in vitro, in vivo and simulated data which is presented below in Section 3.2 and later used for simulation.

3.2 Results

This section discusses the results gathered from the literature review and is divided into four different sections, body type, muscle size, muscle activation and material property values.

3.2.1 Body type

The main criteria which were looked at when checking muscle properties were BMI and gender. A majority of sources noted no major difference of tissue property in either case. Chen Y, et al. [14] conducted a study in which intra-abdominal pressure (IAP) was studied in correlation to AWT which was defined as force to create displacement (N/mm). The study was conducted with patients in the intensive care unit (ICU) at the Shanghai Tenth People's Hospital. To measure the AWT they used a device which they build that could measure the force displacement relation. The study was conducted on 28 male and 23 female ICU patients with BMIs ranging from 15.6-38.6 km/m^2 . The results of this study showed that there was no clear correlation between AWT and gender or BMI.

Another study conducted in the Netherlands by Van Ramshorst G. H. et al. called *Noninvasive Assessment of Intra-Abdominal Pressure by Measurement of Abdominal Wall Tension* [15], also studied different body types. 14 corpses were studied as well as on 42 healthy volunteers where IAP was measured five times at six different points in three different positions whilst doing different exercises. This study, used a prototype for measuring AWT similar to the one Chen Y, et al. used. When the corpses were studied the abdomen was insufflated with air to achieve an IAP from 5mmHg up tp 20mmHg and the AWT was measured at several different points. The healthy volunteers were chosen in an attempt to create a diverse subject group with different genders and BMIs. The group ended up consisting of 22 females and 20 males with BMIs ranging from 16.9 up to 28.1 km/m^2. The results of this study showed that BMI did not influence AWT significantly but that gender could influence the results , with men having levels of AWT which were 31% higher on average. This study also showed that depending on where the measurement was done on the abdomen would influence the AWT value.

3.2.2 Material property values

As mentioned in the data gathering Section 3.1, several different cases were looked at, both in vitro and in vivo and also different models found in the material models 2.2.2 section. Since this study looked at both active and passive muscles these different cases are presented below.

A method for a mechanical characterisation of human gluteal tissue by Then C. et al. [16] studied the stress-strain relation of passive gluteal tissue on a volunteer. The experimental set-up consisted of a Magnetic resonance imaging of the subject whilst an indenter presses in against the buttock with fixed loading and unloading force. The indenters head had a cylindrical shape with a radius of 12.5mm and was equipped with a force transducer of 200N. The person was in a relaxed position, ergo the passive muscle tissue parameters were obtained. The indenter went from displacement values of 0mm up to 10mm in increments with a hold period in between to ensure the force that was needed, the resulting graph can be seen in Then C. et al. *A method for a mechanical characterisation of human gluteal tissue* page 389 [16]. The MR imaging data was then used to separate the different tissues like skin, fat and muscle and their different displacements. Then C. et al. determined that the original thicknes at the place of displacement was 58mm for the muscle tissue and that the skin/fat layer was 32mm. A three dimensional (3D) FE model was created with these values, also including the pelvic bone. The created models were of both the original relaxed and the deformed buttock. The models were meshed and divided into two, one containing the skin/fat layer and another containing the muscle/bone complex. The test showed characteristics of viscoelastic material and Then C. et al. chose to to use a hyperelastic model similar to the Ogden model (more information about the Ogden model can be found under Material models 2.2.2). The Poisson´s ratio ν was set to 0.495 and the parameters for muscle in the ogden model were optimized and set to $\alpha_1 = 0.1316402E + 1$, $\alpha_2 = -0.1835933E + 2$, $\mu_1 = 0.102571E - 2$, $\mu_2 = 0.145209E - 6$, $D_1 = 0.194987E + 2$ and $D_2 = 0.166315E + 3$. The model was simulated and verified comparing the results to the in vivo tests and a correlation factor where $R^2 = 0.997$ was found.

Then C. was included in another study based on *A method for a mechanical characterisation of human gluteal tissue* that was called *Method for characterizing viscoelasticity of human gluteal tissue* [17]. This project was similar in its method and the similar set up was used. Then C. et al. Also used a stepwise indentor and the muscle tissue was also relaxed in this testing [17]. The results were plotted and filtered in order to fit model parameters to match the curve. The main difference between these two studies is that the choosen material model to use in this project was the Hopzafel-Gasser-Ogden which is a variation of the Ogden model used previously. Hopzafel-Gasser-Ogden is used for slightly compressible materials where all the other material models looked at in this study is nearly incompressible. Equation 3.1 shows the stress-strain function where $\bar{w}(\bar{C}, H_i)$ is the deviatoric part (whithout volumetric change) and f(J) represents the volumetric part.

$$w(C, H_i) = \bar{w}(\bar{C}, H_i) + f(J) \tag{3.1}$$

$$\bar{w}(\bar{C}, H_i) = c_1(\bar{C}_1 - 3) + w_f(\bar{C}, H_i) \tag{3.2}$$

$$f(J) = \frac{1}{D}\left[\frac{1}{2}(J^2 - 1) - lnJ\right] \tag{3.3}$$

The second part of the $\bar{w}(\bar{C}, H_i)$ which is the $w_f(\bar{C}, H_i)$ can be written as equation 3.4

$$w_f(\bar{C}, H_i) = \frac{k_1}{2k_2}\sum_{i=1}^{N}(e^{k_2 E_i^{-2}} - 1) \tag{3.4}$$

This equation is a combination of the Neo-Hookean material model, the first part $c_1(\bar{C}_1 - 3)$ and then a second part which can be seen in equation 3.4. The final equation when putting equation 3.1, 3.2, 3.3 and 3.4 together and making some assumptions is equation 3.5

$$w(\bar{C}) = c_1(\bar{C}_1 - 3) + \frac{k_1}{2k_2}\left[e^{(k_2/9)(\bar{I}_1 - 3)^2} - 1\right] + \frac{1}{D}\left[\frac{1}{2}(J^2 - 1) - lnJ\right] \tag{3.5}$$

c_1, D, k_1 and k_2 are material parameters which were fitted in the study with the experimental result data. A model representing the volunteer was created and meshed with second order tetrahedral continuum elements and the parameters obtained from simulating the deformation where $c_1 = 4.40712E - 004$, $D = 2.58623E + 001$, $k_1 = 1.30769E - 002$ and $k_2 = 4.68772E + 001$.

When looking at active tissue there was a limited amount of studies which had been conducted. Many of them either has not published parameter values that can be used, they have created there own models which is very hard to compare with other material model values or there is simply missing values. Most sources also uses values from animals or cadavers which were not taken into consideration in this study [18]. But a study conducted by Fougeron N. et al. [18] looks into the different material properties of the thigh during passive and active muscle stiffness in vivo. Fougeron N. et al. Also create a FE HBM to simulate the results from their study. The study included six men and one women with BMIs ranging from $21.4kg/m^2$ up to 24.3 kg/m^2. The experimental setup used a indentor, a 200N force sensor and a ultrasound probe, more details can be found in their article [18]. The tissue data was acquired in two different positions, one relaxed and one tense where the subject had to lift their own legs, an illustration of this can be seen on page 3, Figure 1 of their article *Combining Freehand Ultrasound-Based Indentation and Inverse Finite Element Modeling for the Identification of Hyperelastic Material Properties of Thigh Soft Tissues* [18]. There were ten loading and unloading cycles for each configuration three times by two operators. The first half of the cycles were conducted in order to assure good preconditioning to make sure the next five could be used for the result. 14 FE models were created, two for each subject, one for each configuration, this was done in ABAQUS FEA (ABAQUS FEA, Inc., Providence, RI). The indentor was simulated and pressed into the models. The soft tissue (Fat and muscle) was simulated using one homogeneous material and the sizes were personalised for each model. The soft tissues material properties were created using the Ogden hyperelastic material model. Where the parameter D was calculated using equation 3.6

$$D = \frac{2}{\kappa} \approx \frac{3(1-2\nu)}{\mu(1+\nu)} \tag{3.6}$$

The parameters were then optimized and used in the models. The parameters can be found in the second page of the article *Combining Freehand Ultrasound-Based Indentation and Inverse Finite Element Modeling for the Identification of Hyperelastic Material Properties of Thigh Soft Tissues* [18].

4 Methods

This thesis was conducted in two parts, the first part being the literature review and the second part involving the simulation of results found in the literature review. The methods were chosen to answer the objectives 1.2 and to answer the main question "Does muscle activity affect a HBM in a significantly?".

In the literature review different studies conducted on muscles around the pelvis and torso was looked at. This would include studies looking at the abdomen, hips, buttocks and the thighs. However before moving on to large muscles and HBM tests the simulations are first done on smaller muscle samples in order to run quick simulations which would generate an idea of what parameters could be used later on. Since the muscle tissue was separated from the body this would also generate more clearly the differences of different muscles and levels of activity and how it affects the muscle tissue once put under an external pressure. The stability of cylindrical model was also analyzed in order to detects errors which occurred once high pressures were used.

The literature study resulted in two different designs which could be used in order to test muscle tissue parameters and weather one could use in vitro data for an in vivo case. The chosen form for this was a simple cylinder to represent a small part of the muscle layer of the body. A positive effect of using a cylinder is that the deformation of the rim is the same around the entire body and there are no errors due to edges which is more similar to how it would look in the body when muscle tissue is deformed, no edges. Later, simulations were also made on an existing avatar. The chosen FE program was ABAQUS FEA and therefore all models found had to have parameters which could be used in this program.

4.1 Cylinder design

The cylinder design was created in order to make quick and somewhat easy simulations to compare different muscle tissue values. The design was inspired by the muscle thickness and indentor size found in Then C. et al. *A method for a mechanical characterisation of human gluteal tissue* [16]. The muscle thickness was reported to be 58mm which was used as the height of the cylinder and the diameter of the cylinder was the same as the probe size which was 25mm. The resulting cylinder was meshed and can be seen in Figure 4.1.

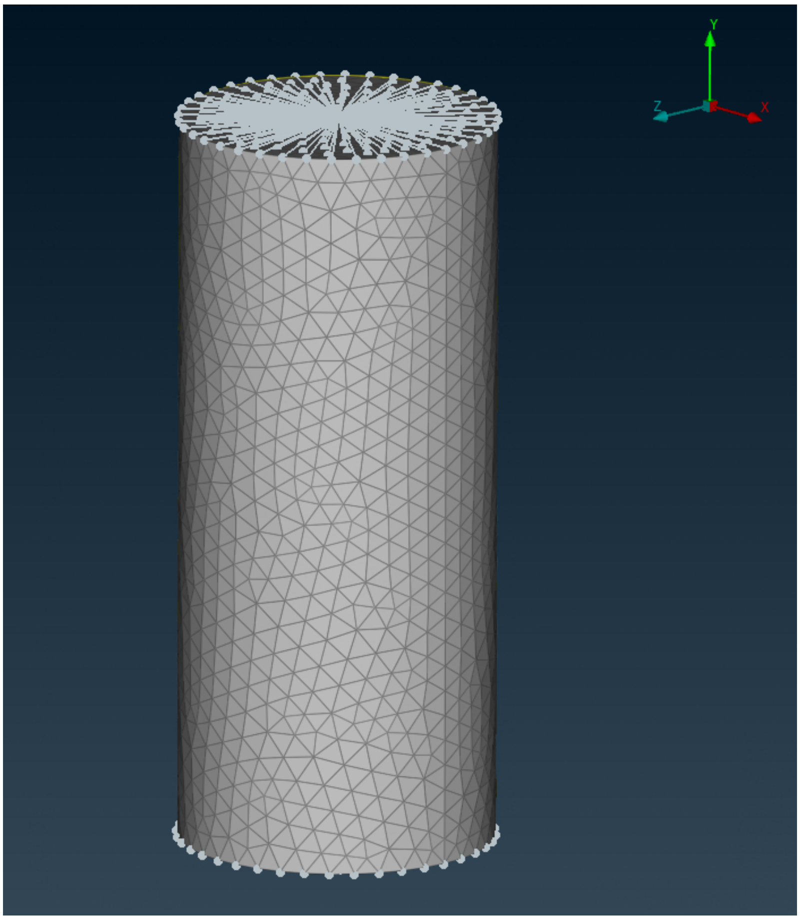

Figure 4.1: Cylinder designed and meshed with Then C. et al. study *A method for a mechanical characterisation of human gluteal tissue*, muscle size as inspiration. In the upper right corner a small working plane can be seen, green points towards y-direction, blue towards z-direction and red towards x-direction.

Another cylinder was also designed to replicate in vitro test studies, the same diameter was kept in order to have comparable results to the in vivo case seen above. The height of this cylinder was set to 7mm in order to replicate the muscle thickness reported in *Mechanical and histological characterization of the abdominal muscle. A previous step to modelling hernia surgery* by Hernández B. et al. [19]. The resulting cylinder is meshed and can be seen in Figure 4.2.

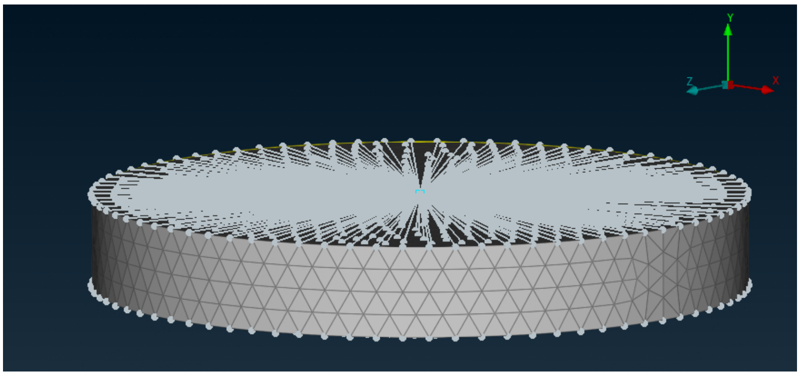

Figure 4.2: Cylinder designed and meshed to imitate in vitro studies with design inspiration from Then C. et al. study *A method for a mechanical characterisation of human gluteal tissue* and Hernández B. et al. study *Mechanical and histological characterization of the abdominal muscle. A previous step to modelling hernia surgery*. In the upper right corner a small working plane can be seen, green points towards y-direction, blue towards z-direction and red towards x-direction.

The cylinders where top and bottom were connected to one master point each in the middle of the circles where the movement of the cylinder could be controlled. The bottom layer was set as fixed in all degrees of freedoms and the top was fixed except in the y-direction (longitudinal plane), in order to stop rotation and movement in the horizontal plane. The master node of the top of the cylinder was then set to move downwards.

4.2 HBM

When the muscle parameters had been tested on the cylindrical shape they were also tested in an existing HBM avatar which was used in order to test different muscle parameters in a human model. This HBM was created with different layers for the different types of tissue such as bone, organs, muscle, fat and skin. The muscles are modeled as one continuous layer throughout the model and the material properties of this layer is the only thing that was edited. The model was then exposed to to elastic bands around the pelvic area, similarly to wear a diapers elastic bands would be.

5 Simulation

The simulations were done in three different phases, the first being the in vitro vs in vivo test case to see if they could be directly translated between each other. The second phase was to test different material properties on the in vivo cylinder to look for similarities between models and values and try to identify usable model values and also look at the difference between the active versus passive muscle isolated. The third phase was then to look at the muscle parameters and their effect in a HBM to se how it affected the real life scenario.

5.1 Cylinder tests

The cylinder tests were done in order to test and verify results from previous studies, the usable muscle materials would then be used in the HBM. The three different studies that were tested can be found in the literature review and corresponding material parameters can be found in Table 6.1. The simulation was done with ABAQUS FEA and the cylinder model was designed in BETA CAE systems ANSA. Once the model was run through ABAQUS FEA it was post processed using BETA CAE systems META where the results were simulated and resulting stress values and graphs could be extracted.

5.1.1 Model verification

Before going into either of the scenarios the model had to be validated to some degree. This was done with a cylinder that had the same muscle material properties as the muscles in Then C. et al. study *A method for a mechanical characterisation of human gluteal tissue* [16] as well as the displacement which was set to 30mm which was the same that can be read in the study. The model was also tested with a second set of parameters from another study by Then C. et al [17] where the model was once again tested to ensure the validity of the model.

5.1.2 Phase 1

In vivo vs in vitro geometry testing

The simulations for the in vitro and in vivo models were run with the exact same material parameters, mesh size and top and bottom area, see under section Cylinder design 4.1. The displacement of each cylinder was set to 20% of the height of each cylinder to try and get the same outcome, the results of this can be seen under

Section 6.2.1. However, what must be taken in to account is the mantle area were the elements in the larger cylinder would have a larger space to get displaced without the element getting to near one another. The two cylinders can be seen in the Cylinder design 4.1 section as Figure 4.1 and Figure 4.2.

5.1.3 Phase 2

Active vs passive muscle tissue and effects of different BMI

Once the model was created and verified the second phase of the simulation part in this projects was to test different muscle tissue. In this part both active and passive muscle tissue was tested for seven different subjects with varying BMI both on their passive and active muscles. The parameter data for this simulation study was taken from the study *Combining Freehand Ultrasound-Based Indentation and Inverse Finite Element Modeling for the Identification of Hyperelastic Material Properties of Thigh Soft Tissues* by Fougeron N. et al. These material properties were put into ANSA on the in vivo cylinder and then run through ABQUS and post-processed with META where the force-displacement could be plotted, seen under Section 6.2.1.

5.2 Human body model test

The HBM test was done for subject 5 in Fougeron N. et al. study *Combining Freehand Ultrasound-Based Indentation and Inverse Finite Element Modeling for the Identification of Hyperelastic Material Properties of Thigh Soft Tissues* [18]. The average BMI of the group was approximately 22.4 kg/m^2 and the closest subject to this value was subject 5 at 22.3. Subject 5 got a force-displacement curve from the cylinder test which was comparatively in the middle of all plots, see Section 6.2.1. Therefor the parameter values used when testing on a HBM was the ones of subject 5. More information about the HBM avatars can be read about in Section 4.2. The Avatars muscle tissue layer was not changed in size, only the material parameter values of the muscles were changed to the ones in subject 5 of Fougeron N. et al. study [18]. The model also contained two elastic bands with three elastic strands each which were simulated to be placed around the groin area around where a diapers elastic bands would be placed. The model was then run through ABAQUS FEA and the results were simulated and analysed in BETA CAE system META.

6 Results

6.1 Literature review

In the literature study resulted in that three main references were used for the simulation part of this project. The result of this can be seen in Table 6.1 where values from three different studies are presented. These muscle tissue parameters (MTPs) will hence forth be called MTP 1, MTP 2 and MTP 3.

Table 6.1: Summarized values of MTPs from three different sources. The first one being an Ogden material model from *A method for a mechanical characterisation of human gluteal tissue* by Then C. et al.. The second one being an Holzapfel-Gasser-Ogden material model by Then C. et al. called *Method for characterizing viscoelasticity of human gluteal tissue.* The third, which also used a Ogden model, called *Combining Freehand Ultrasound-Based Indentation and Inverse Finite Element Modeling for the Identification of Hyperelastic Material Properties of Thigh Soft Tissues* done by Fougeron N. et al..

MTP 1 [16]						
Muscle	μ_1	μ_2	α_1	α_2	D_1	D_2
Gluteal muscles	$0.102571E-02$	$0.145209E-06$	$0.1316402E+01$	$-0.1835933E+02$	$0.194987E+02$	$0.166315E+03$
MTP 2 [17]						
	$c_1(MPa)$	D ($M^{-1}Pa^{-1}$)	$k_1(MPa)$	k_2	κ	
Gluteal muscle	4.41E-004	2.59E+001	1.31E-002	4.69E+001	1/3	
MTP 3 [18]						
Subject	BMI	Relax/Tense (R/T)	μ(kPa)	α	D (v=0.49)	
1	21.4	R	1.86	10	0.02164971	
		T	13.98	3	0.00288043	
2	21.8	R	4.33	11	0.00929987	
		T	9.25	7	0.00435335	
3	21.8	R	2.00	10	0.02013423	
		T	12.88	10	0.00312643	
4	21.7	R	3.43	8	0.01174007	
		T	7.31	12	0.00550868	
5	22.3	R	4.31	11	0.00934303	
		T	11.93	10	0.00337539	
6	23.8	R	1.36	8	0.02960916	
		T	29.36	10	0.00137154	
7	24.3	R	3.91	9	0.01029884	
		T	15.33	12	0.00262677	

Another valuable result was the amount of sources excluded and the in vitro and in vivo results which were used interchangeably. To test whether one could use these sources interchangeably another simulation study was done. More parameters that were looked at can be found in Appendix A.1 unfortunately these values could not be simulated due to missing parameter values or equations which could not be used in ABAQUS FEA.

6.2 Simulation

The simulations were done in several different phases and with different tissue material parameters and models this section is divided into the Cylinder part of the study, the HBM part and then a comparative study between the result found and other results found in the literature review.

6.2.1 Cylinder

As mentioned before the cylinder test was done in several phases, this can be seen under Section 5.1 of the report. The first part was the model verification, then the first tests of in vivo versus in vitro model testing, after that the passive versus active muscles and BMI simulations and lastly the HBM tests.

Model verification

The model verification was done by simulating the cylinder with inspiration from Then C. et al. study *A method for a mechanical characterisation of human gluteal tissue* [16]. The cylinder was done with the muscle tissue parameters found in both Table 6.1 MTP 1 and Table 6.1 MTP 2 to verify the credibility of the model. This verification resulted in two graphs, one for each model which can be seen in Figure 6.1

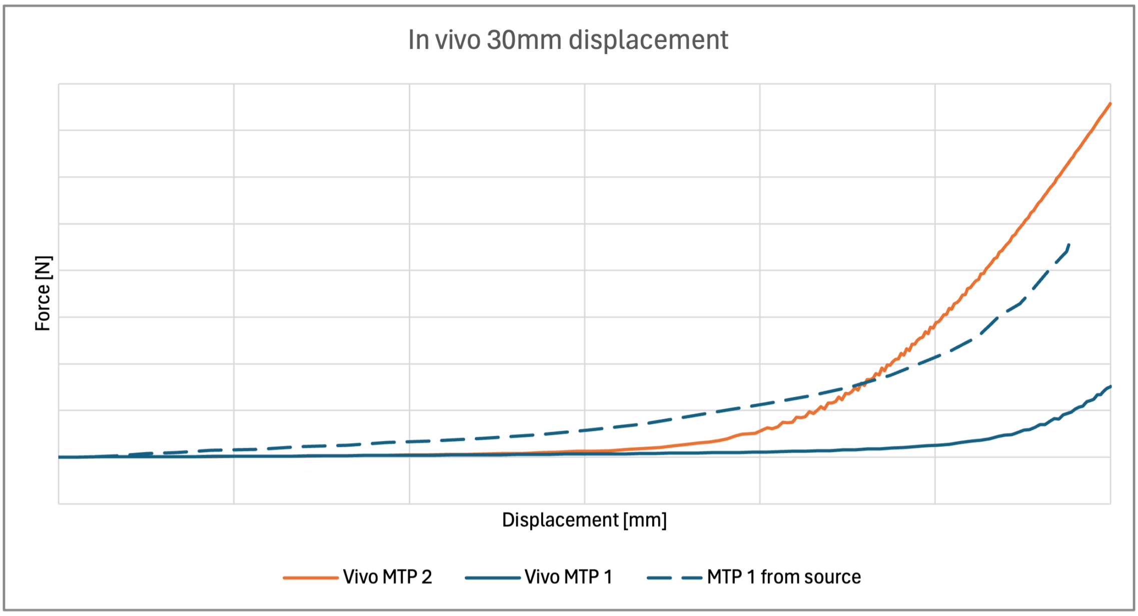

Figure 6.1: The resulting force-displacement curves from 30mm indentation testing on solid muscle where the blue graph is with muscle tissue properties taken from Table 6.1 MTP 1 and the orange graph is with muscle tissue properties from Table 6.1 MTP 2. The dashed line is approximated from *A method for a mechanical characterisation of human gluteal tissue* which is where MTP 1 came from.

When comparing the graph from Then C. et al. study *A method for a mechanical characterisation of human gluteal tissue* on page 391 [16] (or the blue dashed line in this study in Figure 6.1) with the blue graph in Figure 6.1 one can clearly see that there is far less force needed for the same displacement in this simulation. One explanation for this can be seen on the same page as the graph in *A method for a mechanical characterisation of human gluteal tissue* [16] where it is evident that the muscle displacement is not only in the y-direction or localised to the indentors placement. More tissue around the area will also be displaced which therefor needs more force, the fat layer also absorbs some of the force therefor we can see a difference between these to scenarios where in Then C. et al. study a force of approximately 40N is needed for a displacement of the muscle around 30mm whilst in this simulation the required force is only around 15N. The Orange graph which has material properties from the study *Method for characterizing viscoelasticity of human gluteal tissue* by Then C. et al. is much higher which can be explained when looking at the images of the simulation which can be seen in Figure 6.2.

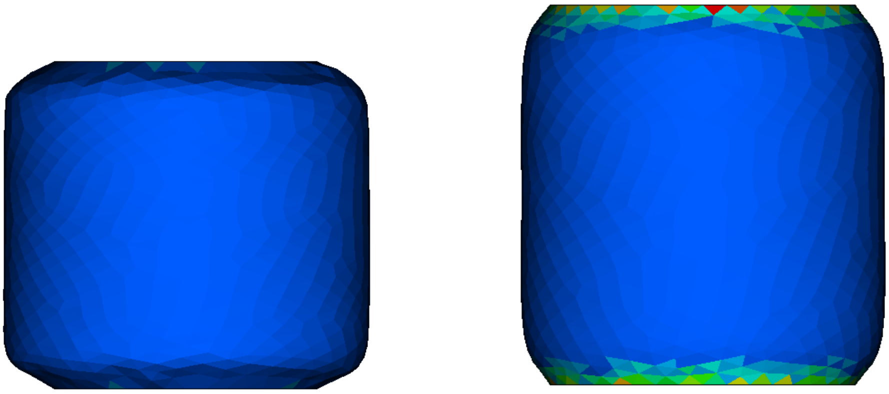

Figure 6.2: The Cylinder to the left is equiped with the muscle tissue parameters found in Table 6.1 MTP 1 and the cylinder to the right is equipped with the muscle tissue parameters found in Table 6.1 MTP 2.

The two figures above are taken after the same amount force in the indentation and clearly the left one, which was from Table 6.1 MTP 1, is lower and easier to deform. This could be because of its non-compressible material properties which makes the cylinder deform more and way less energy which can be stored within the model. The right cylinder with material properties from Table 6.1 MTP 2 is higher and this could be because of its material model which is slightly compressible and therefore a higher force is required to get the same amount of indentation leading to that more is energy stored. This can also be observed in the internal energy plot which can be seen in Figure 6.3.

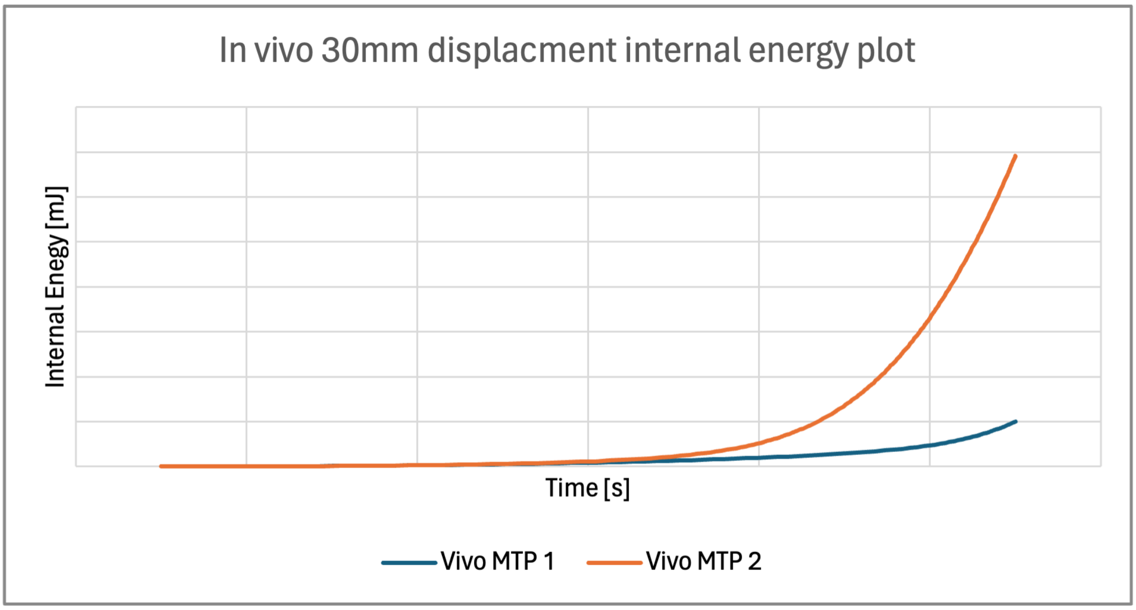

Figure 6.3: The resulting internal energy curves from 30mm indentation testing on solid muscle where the blue graph is with muscle tissue properties taken from Table 6.1 MTP 1 and the orange graph is with muscle tissue properties from Table 6.1 MTP 2.

Since the goal of this study is not to evaluate displacements of this magnitude but rather much smaller magnitude the most important part is that the curves look similar for smaller displacement and energy values which they do.

Phase 1 - In vivo vs in vitro

After the model was verified and working the next step was to test if in vivo and in vitro muscle tissue parameter values could be used interchangeably whilst simulation testing. This was done by using our previous cylinder design with a diameter of 25mm and a height of 58mm with the designed in vitro cylinder which had the same diameter but instead a height of 7mm. More information about cylinder design can be found under Section 4.1 *Cylinder design*. The two cylinders were then set to be indented until a 20% height reduction had been done, this means a 11.6mm displacement for the larger cylinder and a 1.4mm displacement for the smaller one. These tests were run twice with two different sets of muscle tissue parameters, the first was taken from Table 6.1 MTP 1 and the second was taken from Table 6.1 MTP 2. This lead to four runs in total and the resulting force displacement curves can be seen in Figure 6.4.

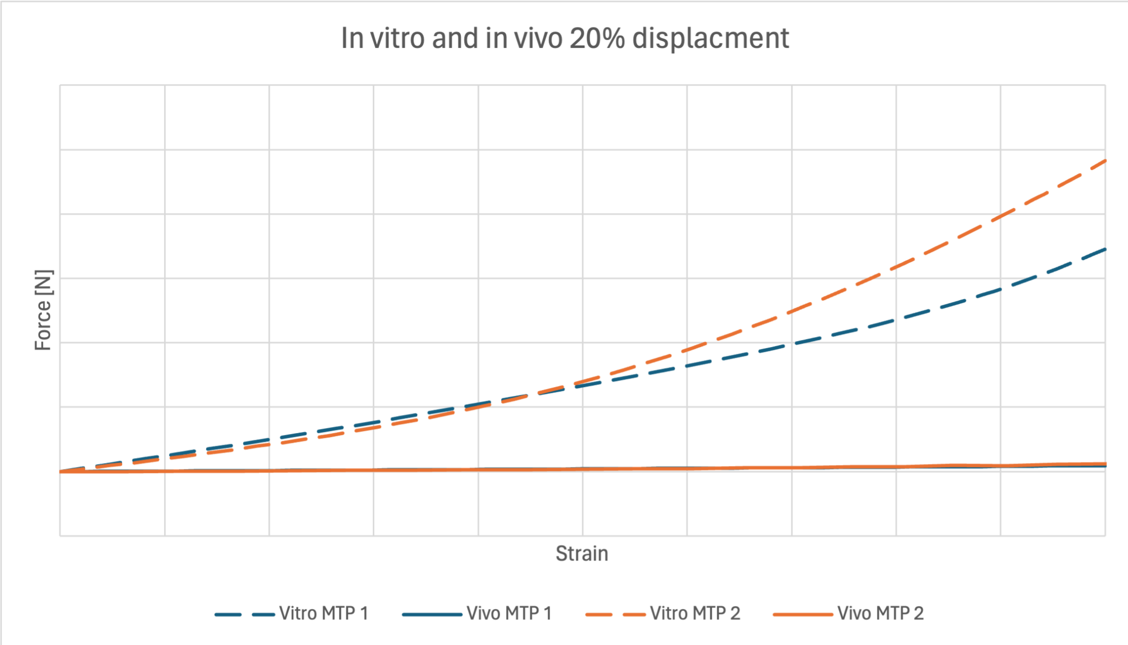

Figure 6.4: The upper two dashed lines is the in vitro design of the cylinder being indented and the bottom two graphs shows the in vivo cylinder being indented. The blue graphs are from muscle tissue parameters found in Table 6.1 MTP 1 and the orange graphs is with the muscle tissue parameters found in Table 6.1 MTP 2.

The strain in 6.4 was calculated by dividing the displacements with initial length of the cylinders. There are some similarities between the curves especially when looking at the general outlook which can be seen when zooming in on the graphs. The orange which is the cylinders with muscle tissue parameters from Table 6.1 MTP 2 is higher in these runs as well as previous. The big difference however is the magnitude of force necessary in order to create a 20% displacement, where the force needed in order to create 20% displacement is very much higher in the in vitro model compared to the in vivo model. A illustration with applied pressure maps of the cylinders during maximum indentation can be seen in Figure 6.5, the pressure goes from dark blue which indicates low pressure to red which indicates high pressure.

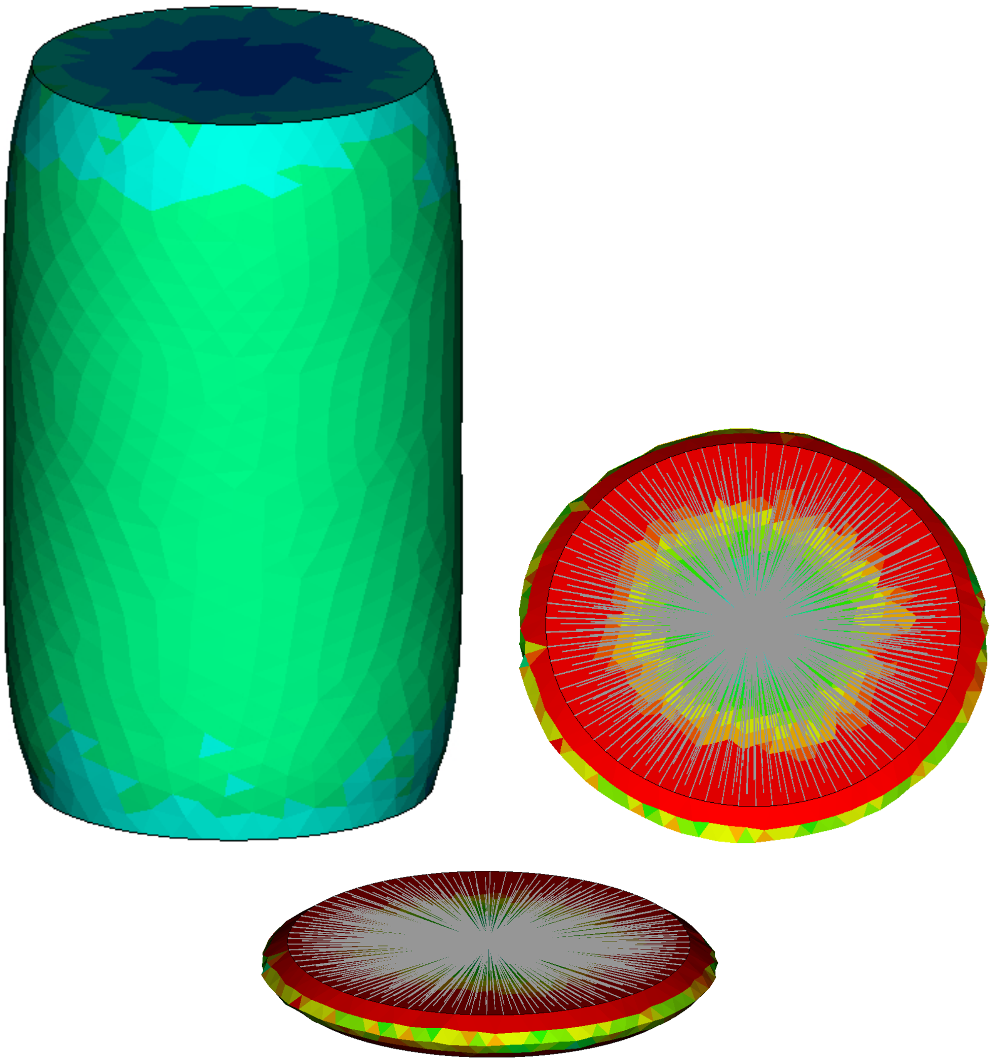

Figure 6.5: The Cylinder to the left is the in vivo cylinder and the cylinder to the right and below is the in vitro cylinder both with muscle tissue parameters found in Table 6.1 MTP 1.

Phase 2 - Active vs passive muscle tissue and effects of different BMI

The next simulations run was to compare active versus passive muscle tissue properties, the muscle tissue parameters used for this study were based on the work by Fougeron N. et al. [18] and applied to the muscle in vivo muscle cylinder created in this project based on the cylinder designed from Table 6.1 MTP 1. A total of 14 runs were done, seven subjects muscle tissue in both active and passive condition of the muscles in the front thigh. The resulting force-displacement curves can be seen in Figure 6.6.

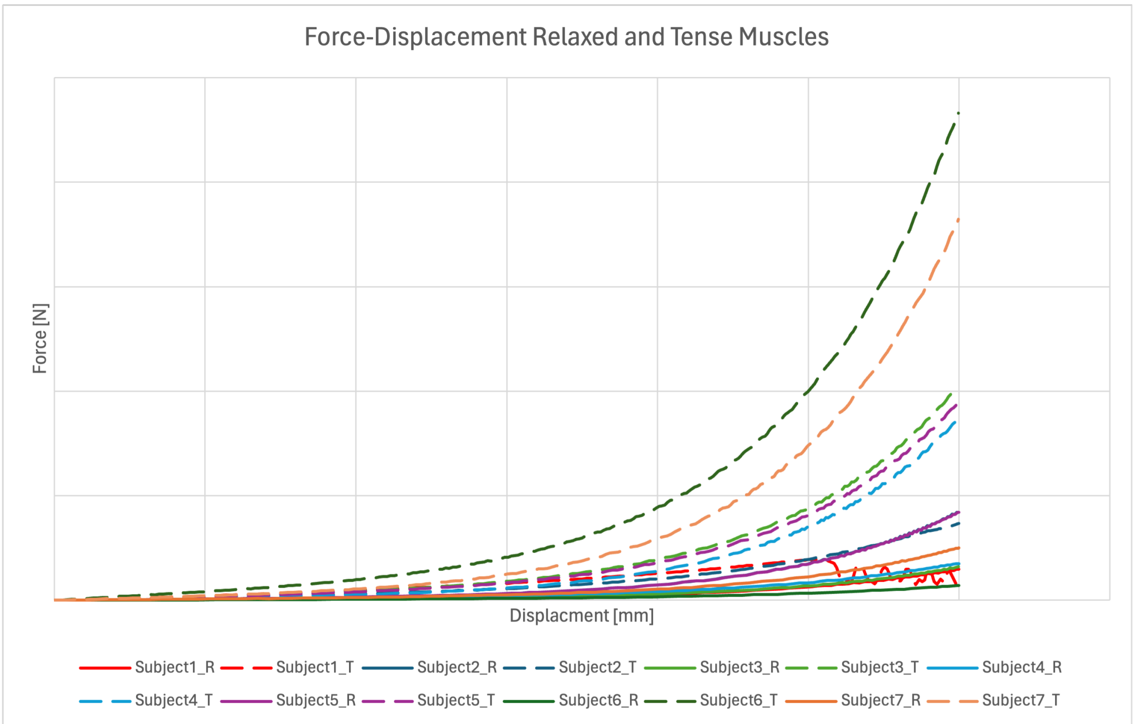

Figure 6.6: Force-displacement plots for all seven subjects with both relaxed (R) and tense (T) muscles. The muscle parameter values are taken from Table 6.1 MTP 3 and the cylinder design inspired from *A method for a mechanical characterisation of human gluteal tissue*. The graphs with tense muscle tissue is illustrated with dashed lines whilst the relaxed tissue is illustrated with solid lines.

Figure 6.6 shows the diversity for muscle tissue values for different subjects where subject six and sevens tense muscles are clearly much higher than the rest of the results. The next graph after these two is the tense values for subject three closely followed by that is the tense values of subject five and then tense values for subject four. Then relaxed result from subject five, tense result from subject two, relaxed subject seven, relaxed subject four, relaxed subject three, relaxed subject one, tense subject one and lastly relaxed muscle value from subject six. All graphs for each subjects can be found in Appendix B.2. The result shows that for almost all subjects a higher force was needed in order to indent the tissue to the maximum displacement, the exceptions for this was for subject one and two. If we look closer at subject one, see Figure 6.7, the graph is clearly distorted, the reason for this distortion is discussed in the discussion Section 7.3.

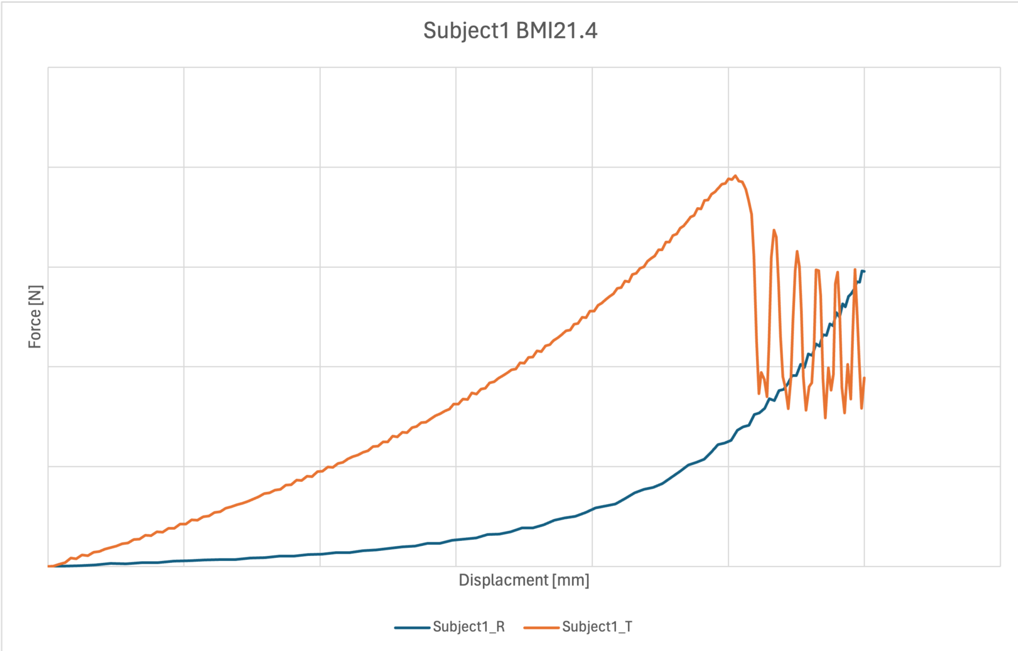

Figure 6.7: Zoomed in force-displacement plots for subject one with both relaxed (R) and tense (T) muscles. The muscle parameter values are taken from Table 6.1 MTP 3 and the cylinder design inspired from *A method for a mechanical characterisation of human gluteal tissue.*

When the simulation images were looked at the error became evident as well, see Figure 6.8, where both cylinders have been distorted to the right in a unnatural way. The right cylinder which is the tense tissue has been unnatural distorted to a much larger extent.

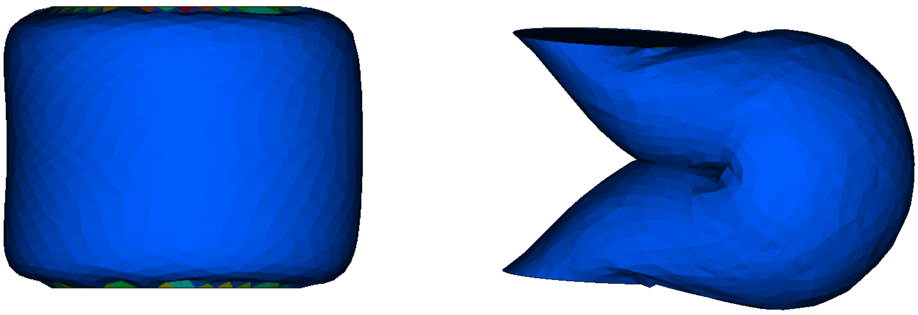

Figure 6.8: The Cylinder to the left is the simulated relaxed muscle tissue of subject one and the cylinder to the right is the simulated tense muscle tissue of subject one both under the maximum amount of indentation. Muscle tissue parameter values are taken from Table 6.1 MTP 3.

However, before the model started to distort unnaturally the curve clearly shows that the tense muscle tissue clearly required a higher force to achieve the same level of indentation. If we then look at a zoomed in graphs of subject two, see Figure 6.9, it is shown that there is a higher force required for the same amount of displacement in the beginning of this plot as well.

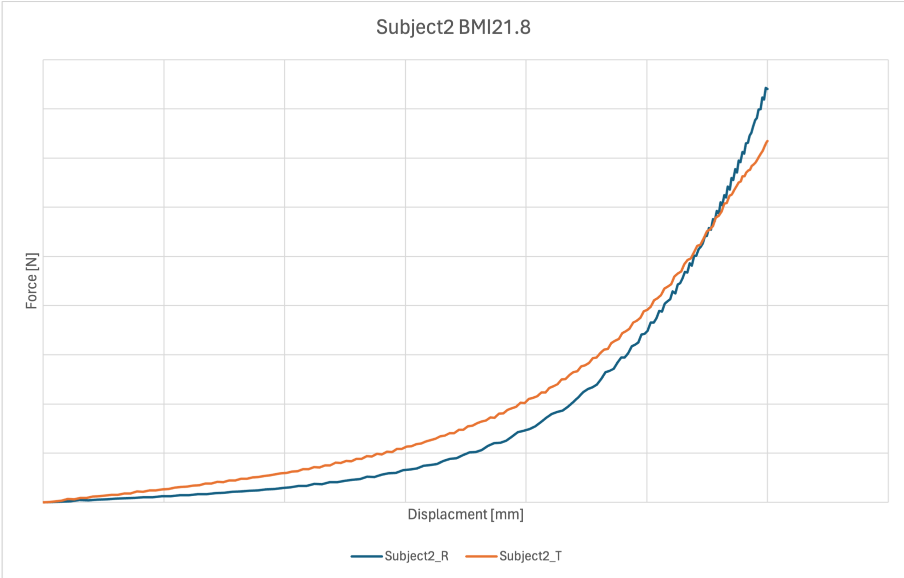

Figure 6.9: Zoomed in force-displacement plots for subject two with both relaxed (R) and tense (T) muscles. The muscle parameter values are taken from Table 6.1 MTP 3 and the cylinder design inspired from *A method for a mechanical characterisation of human gluteal tissue.*

There is no clear distortion of either curve here but in the simulated results, see Figure 6.10, there is a unnatural distortion of the simulated tense muscle tissue cylinder of subject two. The reason for these results will be discussed under Section 7.3.

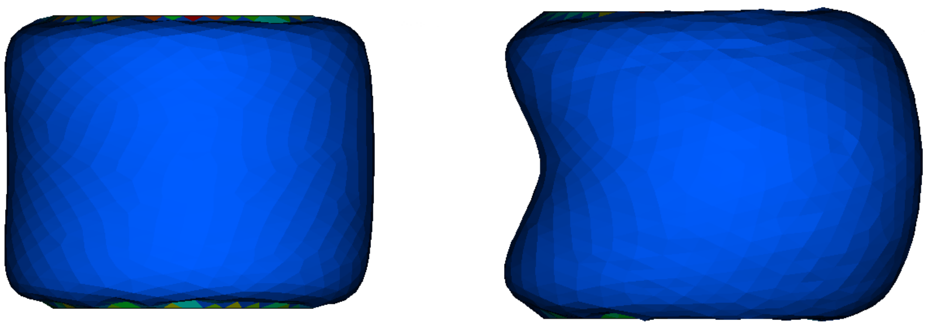

Figure 6.10: The Cylinder to the left is the simulated relaxed muscle tissue of subject two and the cylinder to the right is the simulated tense muscle tissue of subject two both under the maximum amount of indentation. Muscle tissue parameter values are taken from Table 6.1 MTP 3.

6.2.2 Human body model

The anatomy of the HBM avatar was taken from a real person this gives real thickness values and an anatomical accuracy and the tissues were divided into skin, fat, muscle, organ and bone layers. All layers were kept the same with the same parameter data as was used previously in the avatar except for the muscle layer where muscle tissue parameters were changed. The muscle tissue parameters were changed to match subject fives muscle tissue from Table 6.1 MTP 3, more about model design and selection can be found under Section 4.2 and Section 5.2.

The model with the active muscle tissue was slightly more red when simulated which indicated that there was a higher pressure on the body in that model. The passive and active muscle tissue HBM was analysed an there was an almost 7% increase in average pressure from passive to active muscle tissue during the simulation. The data also showed that there was an increase in number of elements in contact in the mesh between the active versus the passive muscle model where there was a 5% increase from active to passive muscle tissue.

7 Discussion

7.1 Method

To fulfil the objectives for this study two different methods were done with different purposes. The first method was a literature review and the second was a simulation study. Both of these methods worked great in order to answer the objectives and complete this project. The project was however time restricted and due to a large amount of misinformation in sources the literature review took longer than expected and the study included an in vitro versus in vivo study in order to see if all sources found could be used which took time away from answering the objectives. There were also some problems with setting up and learning the programs needed for this thesis which also took time.

7.2 Literature review

Early on in the literature study it became apparent that there is a lack of information within the field of stiffness values in the transversal plane for muscles around the pelvis. Many sources refer to studies conducted on animals or cadavers and use them interchanging with human tissue which can not be done in this study. The literature review of reading through sources and finding usable values therefore took a lot longer than planned in order to find correct and usable sources. The second objective could therefor only be answered partly since there was too little information to find on level of activity and how it affects the muscle tissue parameters. Although, the three main sources that were found all have muscle parameter values which were around the pelvis however no sources containing all areas of interest with parameter values in the transversal plane was found. However the sources which were used all contain the necessary parameters and has studies conducted on humans which tests done in the transversal plane and with a diverse group of subjects.

A downside only found in the Fougeron N. et al. article [18] article, was that the fat/muscle layer was merged to one single set of parameters which of course comes with some errors since muscle and fat behave differently. However, the fat layer of the front part of the thigh is very thin, especially when laying down, therefor the study was still used for the simulations.

Despite these shortcomings in the field the results of the literature study were still satisfactory and usable values still came out of it. The study also found several sources which argued for that there was no major differences in muscle tissue parameters between different body types which helped solve objective two. Studies found in Appendix A.1 shows that there is a difference between muscle tissue properties depending on level of activity, sadly these could not be used since the models could not be adapted to ABAQUS FEA.

7.3 Simulation results

The results of the simulations show that there are differences between in vitro and in vivo muscles in a simulatory environment as well as between active and passive muscles. The study also showed that there are no major difference in muscle tissue parameters between different body types. When simulating in the HBM it also became evident that these differences in muscle tissue values also affects the HBM in a simplified product application scenario.

7.3.1 Cylinder

The tests on the cylinders were done in order to gain an insight in the differences when only looking at the muscle tissue. The tests gave a valuable insight in both which studies that were relevant to look at and if there was a difference between active and passive tissue and if it was necessary to do the HBM tests. If the cylinder tests would have given the results that there was no major difference even when isolating the muscle tissue then tests on a HBM avatar would not be necessary. From the model verification it was evident that the cylinder designed from Table 6.1 MTP 1 source could be used in order to test different parameters since it showed similar results as was discovered in MTP 1 and MTP 2 original studies. The in vivo and in vitro testing limited the amount of sources which would be used later to strictly in vivo material parameters since the result from the study showed a great difference between the force-displacement curves for the different geometries. The phase 2 study revealed that there is a difference between active and passive muscle tissue parameters and these parameters could then be used to do more complex simulations in the HBM.

Phase 1 - In vivo vs in vitro geometry testing

This in vivo versus in vitro study was done in order do clarify which results and studies from the literature could be used. If muscle tissue data from animal and cadavers could be used interchangeably to compare results with human data. The results in 6.4 were firstly very surprising since the same percentage of displacement was first theorised to require the same amount of force which was absolutely not the case from these results. This however makes sense once the mantle area of the cylinders is taken into account and Figure 6.5 is looked at. There is far less space for the in vitro cylinder to be displaced over creating both a deformed cylinder which is not even meaning an uneven pressure map and that the elements around the edges would have to be further displaced compared to the in vivo cylinder. However, since there is a clear difference in the force-displacement curves the literature review would not include these results as a comparison to the in vivo models which has been done previously in the field since these values clearly has to be scaled. No studies could be found clarifying the specific difference and how big this difference is between different animals and humans muscle tissue properties. When the study was done with in vitro data the resulting force displacement graphs were not usable, due to a magnitude difference of force which was around 10 000 times higher than all other material parameters used, see Appendix B.1. This could be due to an error with these specific parameters but due to time constraints more data sets were not studied.

Phase 2 - Active vs passive muscle tissue and effects of different BMI

The difference between different BMIs and muscle tissue properties seemed to be pretty insignificant for relaxed tissue. There however seems to be an increase in force necassery to indent tissue for higher BMIs. This is however something which could be explored further with new testing which includes active tissue where there currently is not that much research which has been done.

When looking at the resulting graphs from the active versus passive muscle plots for each individual subject there is a clear trend which showed that a higher force is needed to indent muscles which are active. There are only two exceptions for this phenomenon in this study which was for subject one and subject two. When looking at subject one there is a clear error in the simulation where the active muscle model deformed significantly which made the resulting force-displacement plot derail from what we can assume, based on the other force-displacement plots, that it was going to look like. If the graph would have continued on its course it would have also had a higher value for active muscle tissue. The second subjects cylinder, which also had a lower value for active tissue, can also be seen being more deformed than the passive cylinder which may have corrupted the results. There could also have been an error when measuring the muscle stiffness where the subject might not have been completely relaxed during the first measurements.

That the active muscle tissue would require more force to be indented was expected and from these simulated the next part was to see how big of a difference there was and how much this would affect the human body model.

7.3.2 HBM

The HBM avatar was the same anatomy as a real person and the only thing changed on the avatar in this project was the muscle tissue parameters. The results showed that there is a difference where there is an almost 7% increase in pressure from passive model to the active model. The reason for the higher pressure in the active muscle model could be because the muscles are harder, a larger force is needed in order to move the muscles, this means a larger force with lower displacement leading to a higher pressure on the skin. Higher pressure on the skin leads to higher discomfort for the user wearing the product. How big a difference a 7% increase in pressure makes is hard to tell from just this simulation but this study has shown that there is a difference which should be taken into account when designing and simulating the HBM.

8
Conclusion

In conclusion the objectives of this study has been answered to some degree. The first objective which was "Literature review on how stiffness in muscles changes with level of activity. This includes looking into articles that have studied and modelled active muscles in FE." This was done in the literature review section of the project where several studies were looked at and different models were compared and chosen for the study. The second objective which was "Literature study on how level activity in muscles changes depending on body position and body type." was partly done to the extent which was possible in this project. There was a clear lack of information about how body positioning affected stiffness values in the transversal plane but a study on how active versus passive muscle tissue parameters differed was done and different body types were looked at, although less then originally intended due to the lack of references. The body type studied could also be extended and more testing could be done since the literature review revealed that there should not be a difference between BMIs but the simulation result showed that with a higher BMI the force required was higher. This could of course be due that the parameters composed of both muscle tissue and fat tissue parameters together which again showed the lack of studies and references which were available. The third objective which was to "Simulate a product user interaction case with passive and active muscles and study the differences in a HBM" was done both on isolated muscle tissue and in a HBM which was analyzed.

In the study it was concluded both in the cylindrical and in the HBM tests that there is a clear difference when looking at active versus passive muscle tissue which can be used when looking at product-user interactions in the future. The cylindrical model did a good job of doing quick simulations in order to test material parameters and get an idea of how it will affect a HBM. There is however a lack of information available and a gap within the field that actually study that human body during different activity especially when looking at how it affects the stiffness in the transversal plane. More studies will therefor have to be conducted once more material parameters are available. Muscle tissue can clearly vary between different people and a larger number of sample data could therefore be necessary to give a more definite answer to how much activity and body type affects product-user interaction and force-displacement relations.

For the future of this subject more runs of the HBM could be run with muscle tissue parameters from all the subjects from Table 6.1 MTP 3. Subject fives parameters, which were used in the HBM study, showed a lower difference between active and passive muscle tissue parameters (Figure B.6) than for example subject six (Figure B.7), it would be interesting to see how big of a difference this would make in the HBM. The simulations could also be done with different product types that are of interest in the product-user interactions and also maybe create a in vivo cylinder which is constructed with layers of fat and skin as well to run quick and more accurate simulations. It could also be necessary to conduct a study which measures stiffness values in vivo in the different position that is of interest and then to generate parameters which can be used in ABAQUS FEA.

Bibliography

[1] SIOBHAN AUTY, "What Percentage Of The Population Are Affected By Incontinence?" 12 2023.

[2] "How we test - Diapers," 6 2023.

[3] "Laboratory Testing Services."

[4] R. H. Miller, "Hill-Based Muscle Modeling," in *Handbook of Human Motion*. Cham: Springer International Publishing, 2018, pp. 1–22.

[5] A. Jourdan, R. Dhume, E. Guérin, A. Siegel, A. Le Ruyet, and M. Palmer, "Numerical investigation of a finite element abdominal wall model during breathing and muscular contraction," *Computer Methods and Programs in Biomedicine*, vol. 244, p. 107985, 2 2024.

[6] F. M. Trovato, R. Imbesi, N. Conway, and P. Castrogiovanni, "Morphological and functional aspects of human skeletal muscle," pp. 289–302, 9 2016.

[7] W. Flynn and P. Vickerton, "Anatomy, Abdomen and Pelvis: Abdominal Wall," 7 2023.

[8] A. Osika, "Hip and thigh muscles," *KEN HUB*, 9 2023.

[9] "Physiopedia," 5 2024. [Online]. Available: https://www.physio-pedia.com/Quadriceps_Muscle?utm_source=physiopedia&utm_medium=search&utm_campaign=ongoing_internalhttps://www.physio-pedia.com/Adductor_Magnushttps://www.physio-pedia.com/Hamstrings?utm_source=physiopedia&utm_medium=search&utm_campaign=ongoing_internal

[10] ABAQUS Theory manual, "https://classes.engineering.wustl.edu/2009/spring/mase5513/abaqu

[11] Sai Kosaraju, "https://www.fidelisfea.com/post/hyperelastic-materials-in-abaqus-what-are-they-and-how-do-they-work," 6 2022.

[12] J. Bergström, "Elasticity/Hyperelasticity," in *Mechanics of Solid Polymers*. Elsevier, 2015, pp. 209–307.

[13] H. Djadoudi, "Abaqus Expert Review, Pricing and Alternatives - 2024," 2024. [Online]. Available: https://www.worquick.com/post/abaqus-review

[14] Y.-z. Chen, S.-y. Yan, Y.-q. Chen, Y.-g. Zhuang, Z. Wei, S.-q. Zhou, and H. Peng, "Noninvasive monitoring of intra-abdominal pressure by measuring abdominal wall tension," *World Journal of Emergency Medicine*, vol. 6, no. 2, p. 137, 2015.

[15] G. H. Van Ramshorst, M. Salih, W. C. Hop, O. J. Waes, G. J. Kleinrensink, R. H. Goossens, and J. F. Lange, "Noninvasive assessment of intra-abdominal pressure by measurement of abdominal wall tension," *Journal of Surgical Research*, vol. 171, no. 1, pp. 240–244, 11 2011.

[16] C. Then, J. Menger, G. Benderoth, M. Alizadeh, T. Vogl, F. Hübner, and G. Silber, "A method for a mechanical characterisation of human gluteal tissue," *Technology and Health Care*, vol. 15, no. 6, pp. 385–398, 12 2007.

[17] C. Then, T. J. Vogl, and G. Silber, "Method for characterizing viscoelasticity of human gluteal tissue," *Journal of Biomechanics*, vol. 45, no. 7, pp. 1252–1258, 4 2012.

[18] N. Fougeron, P. Y. Rohan, D. Haering, J. L. Rose, X. Bonnet, and H. Pillet, "Combining Freehand Ultrasound-Based Indentation and Inverse Finite Element Modeling for the Identification of Hyperelastic Material Properties of Thigh Soft Tissues," *Journal of Biomechanical Engineering*, vol. 142, no. 9, 9 2020.

[19] B. Hernández, E. Peña, G. Pascual, M. Rodríguez, B. Calvo, M. Doblaré, and J. M. Bellón, "Mechanical and histological characterization of the abdominal muscle. A previous step to modelling hernia surgery," *Journal of the Mechanical Behavior of Biomedical Materials*, vol. 4, no. 3, pp. 392–404, 4 2011.

[20] L. Astruc, M. De Meulaere, J. F. Witz, V. Nováček, F. Turquier, T. Hoc, and M. Brieu, "Characterization of the anisotropic mechanical behavior of human abdominal wall connective tissues," *Journal of the Mechanical Behavior of Biomedical Materials*, vol. 82, pp. 45–50, 6 2018.

[21] S. Todros, N. de Cesare, G. Concheri, A. N. Natali, and P. G. Pavan, "Numerical modelling of abdominal wall mechanics: The role of muscular contraction and intra-abdominal pressure," *Journal of the Mechanical Behavior of Biomedical Materials*, vol. 103, 3 2020.

[22] A. Tomaszewska, I. Lubowiecka, and C. Szymczak, "Mechanics of mesh implanted into abdominal wall under repetitive load. Experimental and numerical study," *Journal of Biomedical Materials Research - Part B Applied Biomaterials*, vol. 107, no. 5, pp. 1400–1409, 7 2019.

A

Appendix A

A.1 Stiffness values

These are the tables that were not used in the study but shows great potential for the development in the field.

Table A.1 was not used due to the lack of understanding of the parameters since they do not match with the parameters used in the Holzapfel-Gasser-Ogden model. The parameters are taken from a study conducted by Jourdan a. et al. [5].

Table A.1: Different levels of activity in abdominal muscles and the Holzapfel-Gasser-Ogden material parameters

Muscles (Passive)	Holzapfel-Gasser-Ogden			
	μ_1	α_1	k_{11} (Pa)	k_{21} (Pa)
Rectus Abdominis (+)	5000	6	55000	0.01
Rectus Abdominis	3000	5.5	45000	0.01
Rectus Abdominis (-)	2200	5	30000	0.01
External Oblique (+)	10000	5	20000	1.1
External Oblique	4000	5.5	12000	1.1
External Oblique (-)	2200	5	5000	1.1
Internal Oblique (+)	10000	4.3	20000	0.01
Internal Oblique	8000	4	15000	0.01
Internal Oblique (-)	6000	4	10000	0.01
Transversus Abdominis (+)	15000	5	85000	0.01
Transversus Abdominis	6000	5	60000	0.01
Transversus Abdominis (-)	2200	4	30000	0.01

Table A.2 was not used since the study done by Astruc L. et al. [20] did not contain the material parameters in order to recreate the study but simply the results.

Table A.2: Summary of Mechanical Properties of Abdominal Tissues

Muscle group	**N**	E_0 **(MPa)**	**E´ (MPa)**	C_1 **(MPa)**	C_2 **(MPa)**
Linea Alba	37	1.2 (1.3)	4.8 (6.0)	0.32 (0.31)	1.3 (1.4)
Anterior Rectus Sheath	102	2.5 (2.3)	11 (7.0)	0.65 (0.68)	2.3 (2.2)
Posterior Rectus Sheath	55	4.2 (6.2)	15 (12)	1.1 (1.1)	4.1 (10)

Table A.3 was not used since the parameters referred to in the table does not match the Ogden model parameters which was used in this study. The parameters where taken from Todros S. et al. study [21].

Table A.3: Mechanical Properties of Various Tissues

Tissue	k_{fv} **[MPa]**	μ_f **[MPa]**	a_{f1} **[MPa]**	a_{f2}
Linea Alba	2000	0.260	0.450	45.68
Aponeuroses	2000	0.260	0.450	45.68
Fasciae	2000	0.020	0.310	7.71
	k_{mv} **[MPa]**		a_{m1} **[MPa]**	a_{m2}
Muscles	1.0	-	0.03	0.9

Table A.4 was not used since it was based on in vitro studies and the D_1 and D_2 parameters for the Ogden model are missing. The parameters were taken from Tomaszewska A. et al. study [22].

Table A.4: Muscle tissue values of the abdomen

Muscle	$\mu_1[N/m]$	$\mu_2[N/m]$	α_1	α_2
abdomen	1.33E-9	87.1	107	11.7

B

Appendix B

B.1 Force-displacement curves in vitro values

Force-displacement curve with muscle tissue parameter values taken from an in vitro study done by Tomaszewska A. et al. [22] and can be found in Figure B.1.

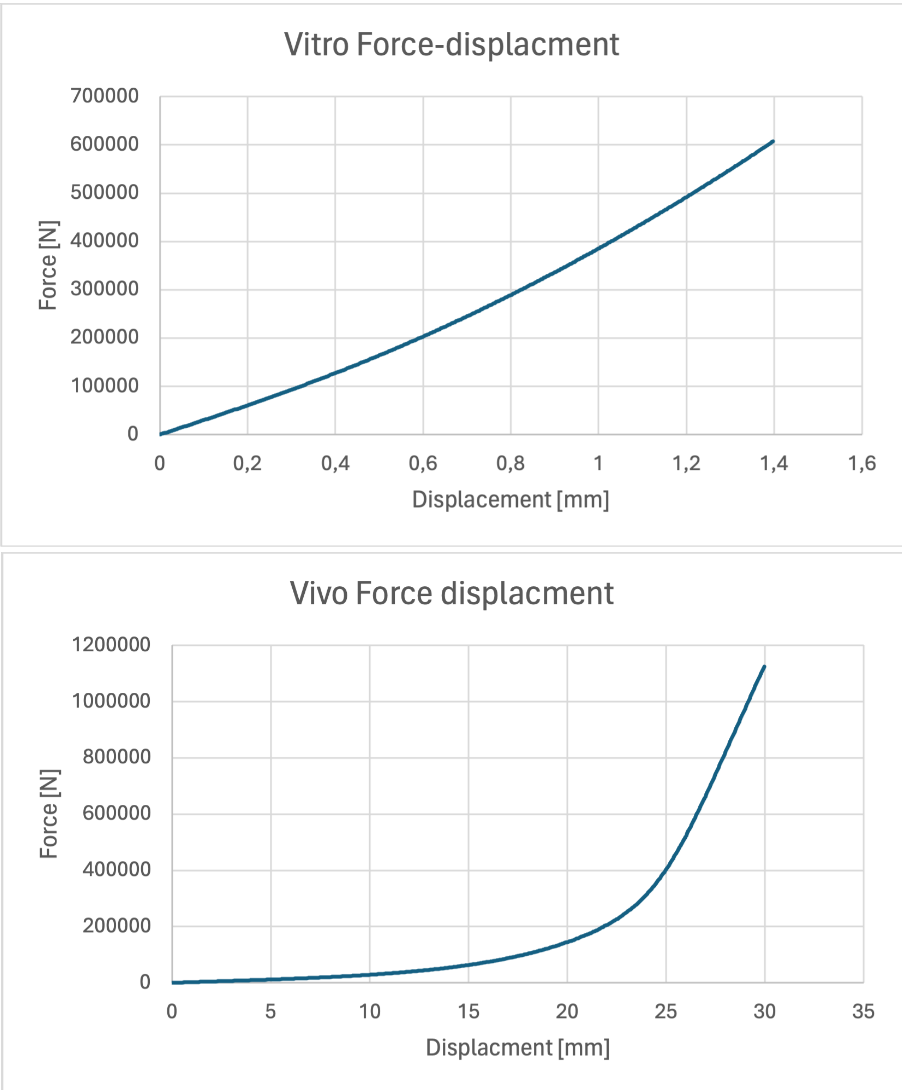

Figure B.1: Force-displacement plots of both in vivo and in vitro cylinder designs with muscle tissue material values taken from Tomaszewska A. et al. study.

B.2 Force-displacement curves Active versus passive muscle tissue values

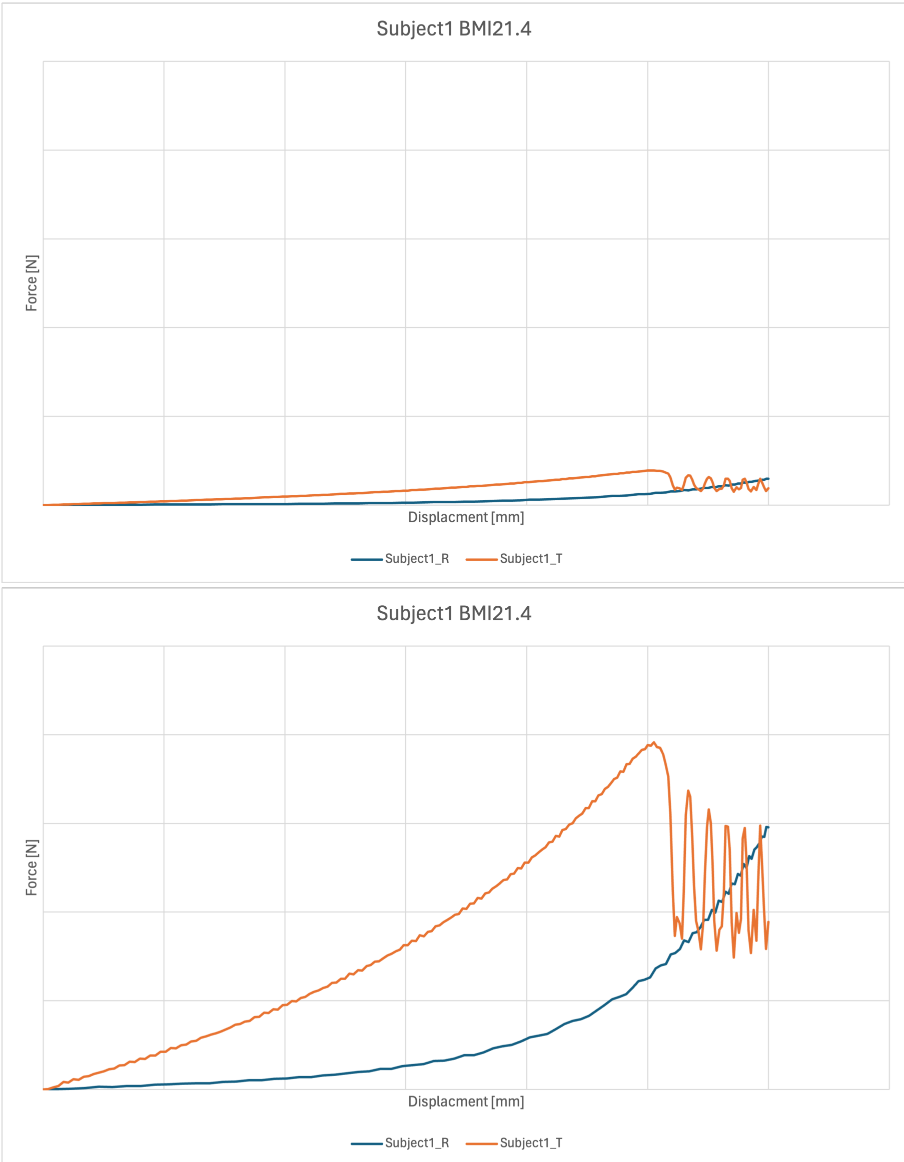

Figure B.2: Force-displacement plots of subject one with both relaxed (R), in blue, and tense (T), in orange, muscles. The muscle parameter values are taken from Table 6.1 MTP 3 and the cylinder design inspired from Then C. et al. study *A method for a mechanical characterisation of human gluteal tissue*. The first image is to scale with all others and the second is zoomed in.

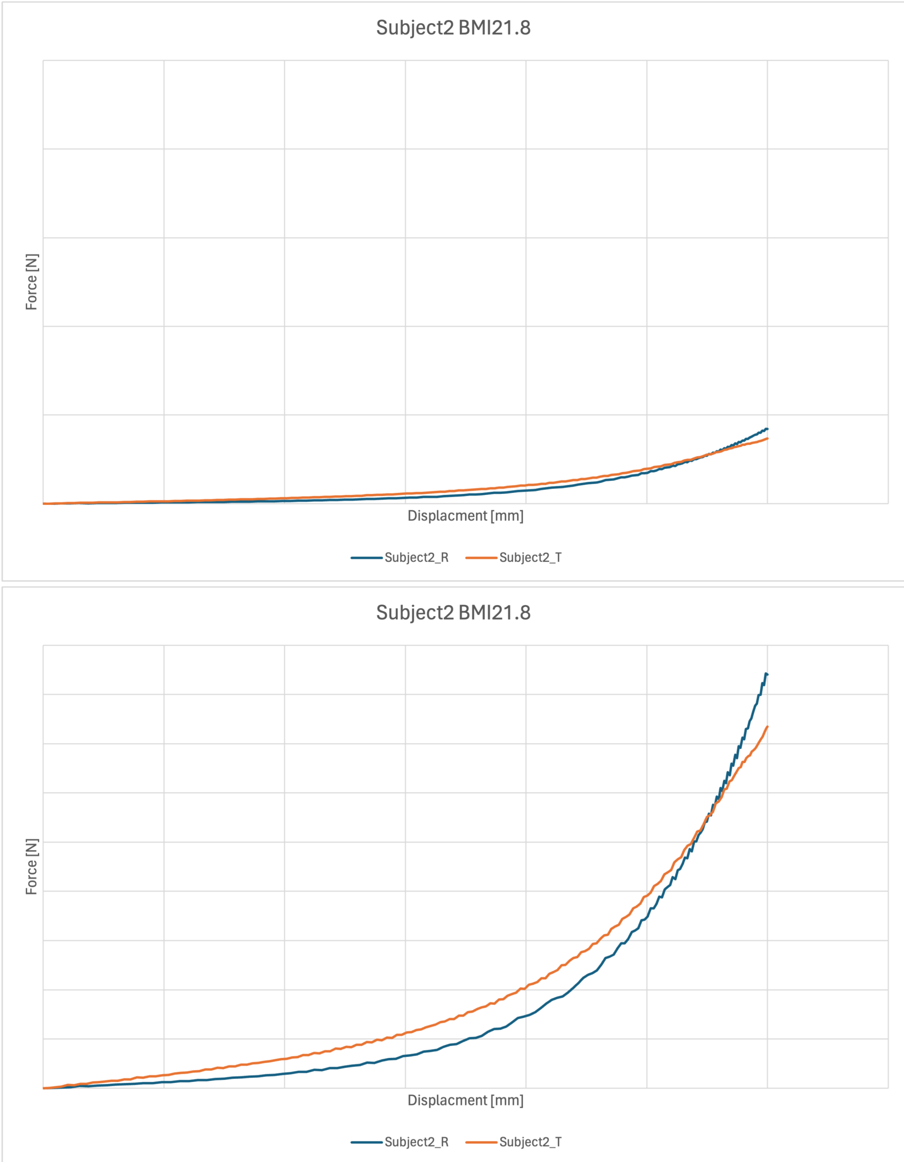

Figure B.3: Force-displacement plots of subject two with both relaxed (R), in blue, and tense (T), in orange, muscles. The muscle parameter values are taken from Table 6.1 MTP 3 and the cylinder design inspired from Then C. et al. study *A method for a mechanical characterisation of human gluteal tissue*. The first image is to scale with all others and the second is zoomed in.

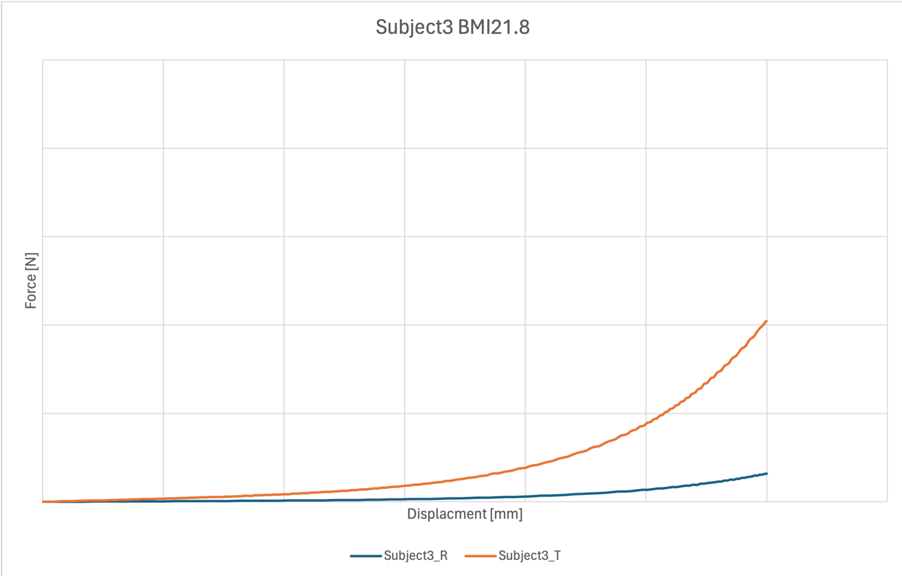

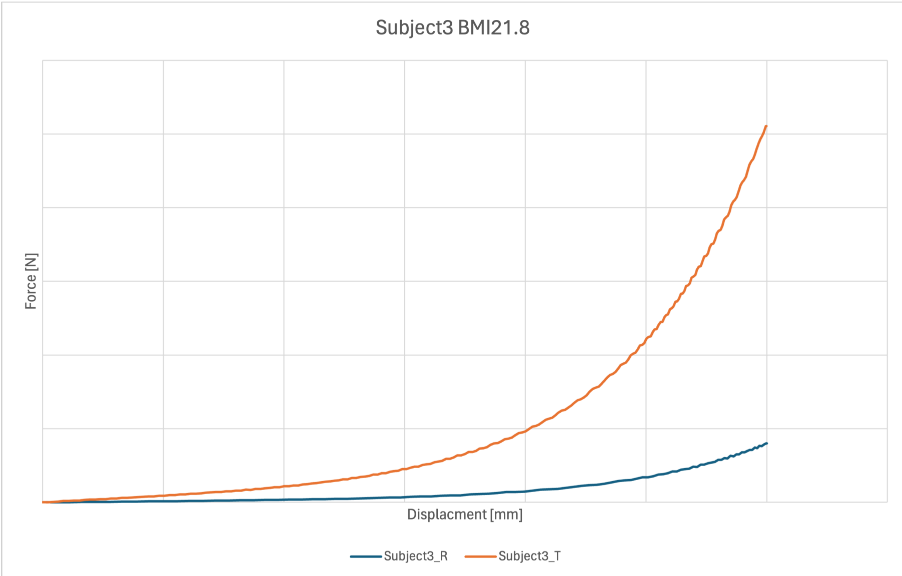

Figure B.4: Force-displacement plots of subject three with both relaxed (R), in blue, and tense (T), in orange, muscles. The muscle parameter values are taken from Table 6.1 MTP 3 and the cylinder design inspired from Then C. et al. study *A method for a mechanical characterisation of human gluteal tissue*. The first image is to scale with all others and the second is zoomed in.

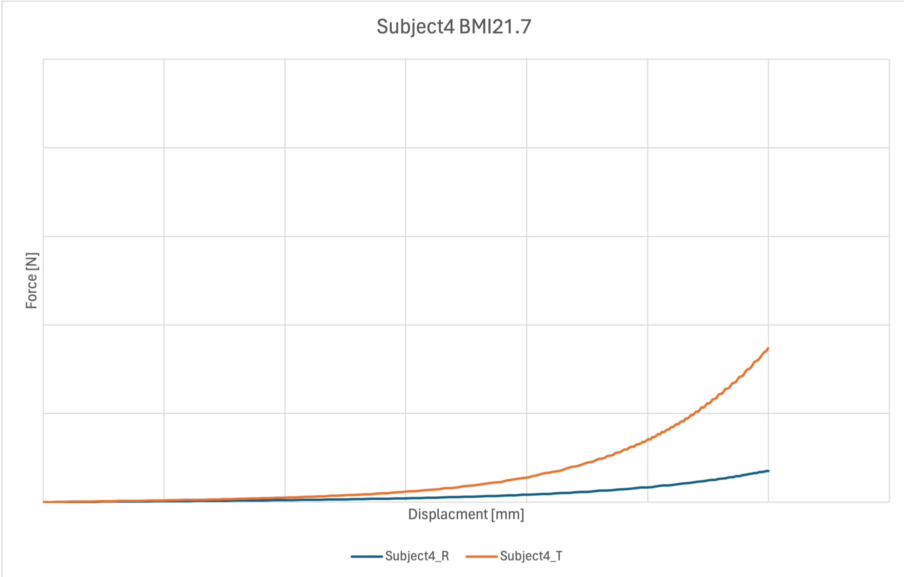

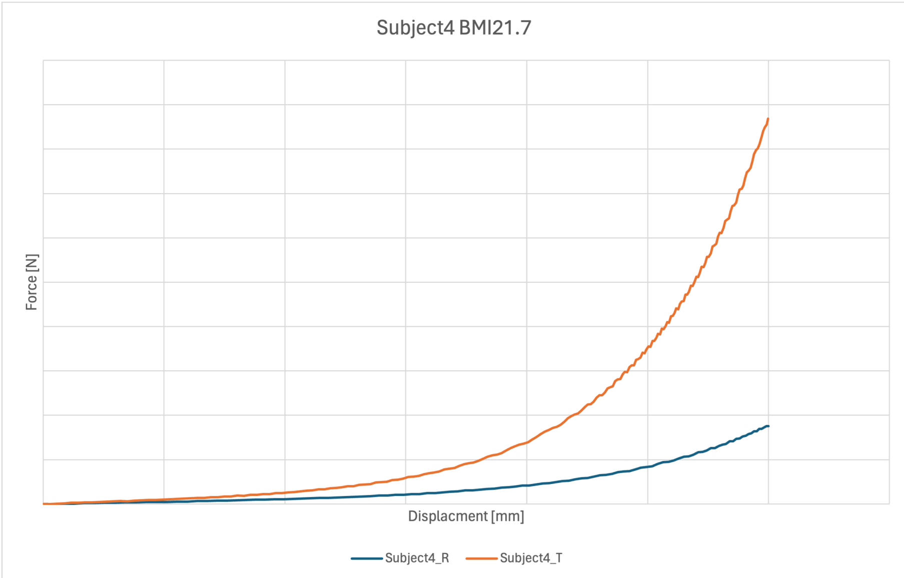

Figure B.5: Force-displacement plots of subject four with both relaxed (R), in blue, and tense (T), in orange, muscles. The muscle parameter values are taken from Table 6.1 MTP 3 and the cylinder design inspired from Then C. et al. study *A method for a mechanical characterisation of human gluteal tissue*. The first image is to scale with all others and the second is zoomed in.

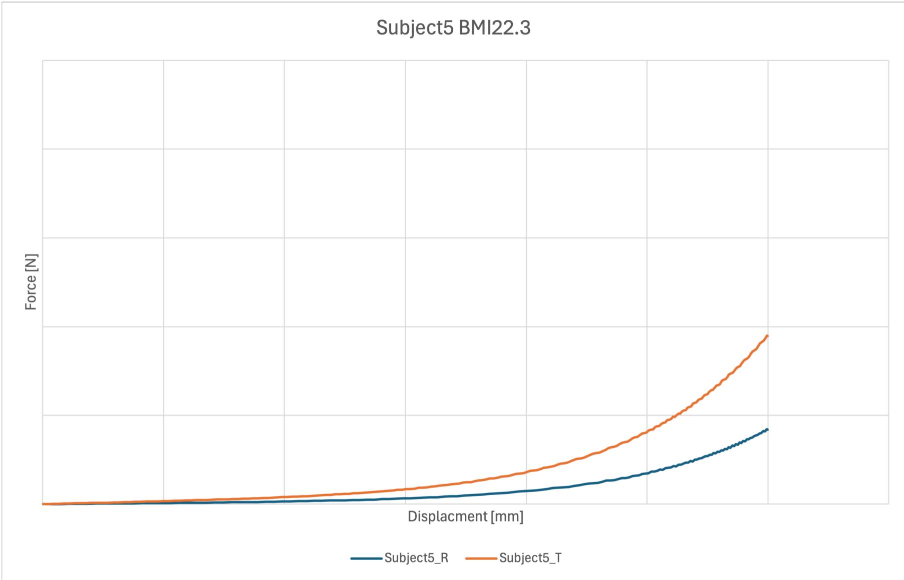

Figure B.6: Force-displacement plots of subject five with both relaxed (R), in blue, and tense (T), in orange, muscles. The muscle parameter values are taken from Table 6.1 MTP 3 and the cylinder design inspired from Then C. et al. study *A method for a mechanical characterisation of human gluteal tissue*. The first image is to scale with all others and the second is zoomed in.

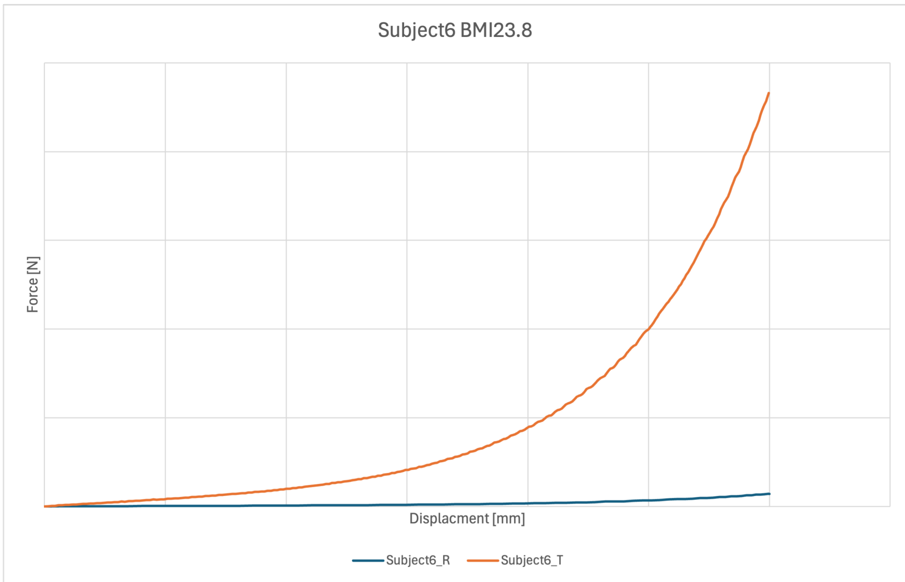

Figure B.7: Force-displacement plots of subject six with both relaxed (R), in blue, and tense (T), in orange, muscles. The muscle parameter values are taken from Table 6.1 MTP 3 and the cylinder design inspired from Then C. et al. study *A method for a mechanical characterisation of human gluteal tissue.*

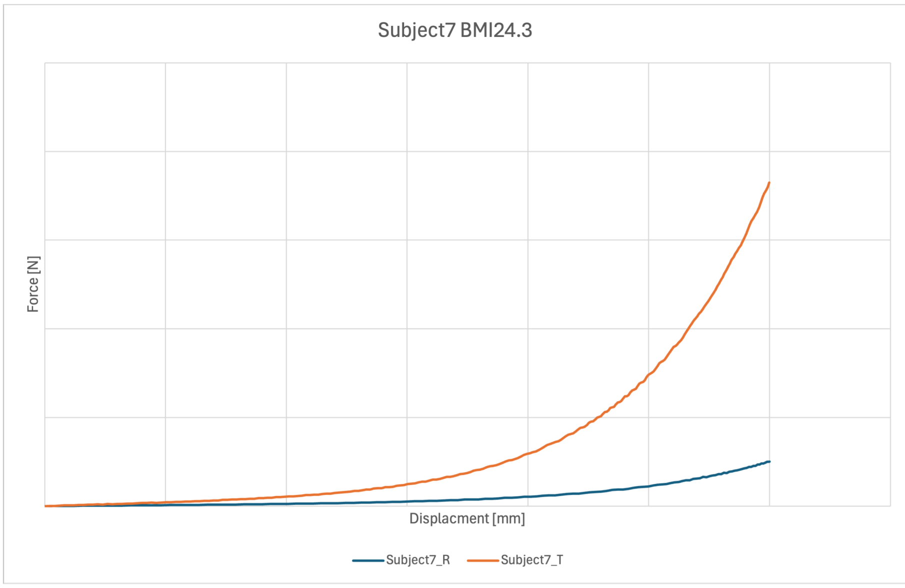

Figure B.8: Force-displacement plots of subject seven with both relaxed (R), in blue, and tense (T), in orange, muscles. The muscle parameter values are taken from Table 6.1 MTP 3 and the cylinder design inspired from Then C. et al. study *A method for a mechanical characterisation of human gluteal tissue.*

DEPARTMENT OF SOME SUBJECT OR TECHNOLOGY
CHALMERS UNIVERSITY OF TECHNOLOGY
Gothenburg, Sweden
www.chalmers.se

CHALMERS
UNIVERSITY OF TECHNOLOGY